



Targeting miR-30d reverses pathological cardiac hypertrophy

Jin Li,^{a,b,1} Zhao Sha,^{a,b,1} Xiaolan Zhu,^{a,b,1} Wanru Xu,^{a,b} Weilin Yuan,^{a,b} Tingting Yang,^{a,b}
 Bing Jin,^{a,b} Yuwei Yan,^{a,b} Rui Chen,^{a,b} Siqi Wang,^{a,b} Jianhua Yao,^c Jiahong Xu,^d Zitong Wang,^e
 Guoping Li,^f Saumya Das,^f Liming Yang,^{g**} and Junjie Xiao^{a,b*}

^aInstitute of Geriatrics (Shanghai University), Affiliated Nantong Hospital of Shanghai University (The Sixth People's Hospital of Nantong), School of Medicine, Shanghai University, Nantong 226011, China

^bCardiac Regeneration and Ageing Lab, Institute of Cardiovascular Sciences, Shanghai Engineering Research Center of Organ Repair, School of Life Science, Shanghai University, Shanghai 200444, China

^cDepartment of Cardiology, Tenth People's Hospital, School of Medicine, Tongji University, Shanghai 200090, China

^dDepartment of Cardiology, Shanghai Tongji Hospital, School of Medicine, Tongji University, Shanghai 200065, China

^eDepartment of Pathophysiology, Basic Medical Science, Harbin Medical University, Harbin 150081, China

^fCardiovascular Division of the Massachusetts General Hospital and Harvard Medical School, Boston, MA 02114, USA

^gDepartment of Pathophysiology, Harbin Medical University-Daqing, Daqing, 163319, China

Summary

Background Pathological cardiac hypertrophy occurs in response to numerous stimuli and precedes heart failure (HF). Therapies that ameliorate pathological cardiac hypertrophy are highly needed.

Methods The expression level of miR-30d was analyzed in hypertrophy models and serum of patients with chronic heart failure by qRT-PCR. Gain and loss-of-function experiments of miR-30d were performed *in vitro*. miR-30d gain of function were performed *in vivo*. Bioinformatics, western blot, luciferase assay, qRT-PCR, and immunofluorescence were performed to examine the molecular mechanisms of miR-30d.

Findings miR-30d was decreased in both murine and neonatal rat cardiomyocytes (NRCMs) models of hypertrophy. miR-30d overexpression ameliorated phenylephrine (PE) and angiotensin II (Ang II) induced hypertrophy in NRCMs, whereas the opposite phenotype was observed when miR-30d was downregulated. Consistently, the miR-30d transgenic rat was found to protect against isoproterenol (ISO)-induced pathological hypertrophy. Mechanistically, methyltransferase EZH2 could promote H3K27me3 methylation in the promotor region of miR-30d and suppress its expression during the pathological cardiac hypertrophy. miR-30d prevented pathological cardiac hypertrophy via negatively regulating its target genes MAP4K4 and GRP78 and inhibiting pro-hypertrophic nuclear factor of activated T cells (NFAT). Adeno-associated virus (AAV) serotype 9 mediated-miR-30d overexpression exhibited beneficial effects in murine hypertrophic model. Notably, miR-30d was reduced in serum of patients with chronic heart failure and miR-30d overexpression could significantly ameliorate pathological hypertrophy in human embryonic stem cell-derived cardiomyocytes.

Interpretation Overexpression of miR-30d may be a potential approach to treat pathological cardiac hypertrophy.

Funding This work was supported by the grants from National Key Research and Development Project (2018YFE0113500 to J Xiao), National Natural Science Foundation of China (82020108002 to J Xiao, 81900359 to J Li), the grant from Science and Technology Commission of Shanghai Municipality (20DZ2255400 and 21XD1421300 to J Xiao, 22010500200 to J Li), Shanghai Sailing Program (19YF1416400 to J Li), the "Dawn" Program of Shanghai Education Commission (19SG34 to J Xiao), the "Chen Guang" project supported by the Shanghai Municipal Education Commission and Shanghai Education Development Foundation (19CG45 to J Li).

*Corresponding author at: Cardiac Regeneration and Ageing lab, Institute of Cardiovascular Sciences, Shanghai Engineering Research Center of Organ Repair, School of Life Science, Shanghai University, 333 Nan Chen Road, Shanghai 200444, China.

**Corresponding author at: Department of Pathophysiology, Harbin Medical University-Daqing, Daqing, 163319, China.

E-mail addresses: limingyanghmu@163.com (L. Yang), junjexiao@shu.edu.cn (J. Xiao).

¹ These authors contributed equally to this work.

eBioMedicine 2022;81:
104108

Published online xxx
<https://doi.org/10.1016/j.ebiom.2022.104108>

Copyright © 2022 The Author(s). Published by Elsevier B.V. This is an open access article under the CC BY-NC-ND license (<http://creativecommons.org/licenses/by-nc-nd/4.0/>)

Keywords: Pathological cardiac hypertrophy; miR-30d; Translational research

Research in context

Evidence before the study

MicroRNA (miRNA, miR) has been shown to have a vital role in cardiovascular diseases including pathological cardiac hypertrophy and heart failure. The authors previously reported that miR-30d regulated adverse cardiac remodeling by intracellular and paracrine signaling. However, if miR-30d could be a therapeutic target for pathological cardiac hypertrophy is undetermined.

Added value of the study

1. miR-30d is significantly decreased in both murine and neonatal rat cardiomyocytes (NRCMs) models of hypertrophy.
2. AAV9-mediated elevation of miR-30d reversed established pathological cardiac hypertrophy *in vivo*.
3. Mechanistically, the EZH2-miR-30d-MAP4K4/GRP78-NFAT signaling pathway appears to be involved in cardiac hypertrophy.
4. miR-30d is reduced in the serum of patients with chronic heart failure and miR-30d overexpression could significantly ameliorate pathological hypertrophy in human embryonic stem cell-derived cardiomyocytes.

Implications of all the available evidence

Our findings indicate that overexpression of miR-30d represents a potential therapeutic intervention for pathological cardiac hypertrophy.

Introduction

Pathological cardiac hypertrophy is a process caused by compensatory response to long-standing biomechanical pressure or volume overload, which is commonly observed in patients with hypertension, myocardial infarction and valvular diseases.¹ Pathological cardiac hypertrophy often precedes overt heart failure and is an independent prognosticator of cardiovascular mortality. Current pharmacological agents including β -blockers, calcium antagonists, or angiotensin-converting enzyme (ACE) inhibitors are largely used after clinical manifestation of HF symptoms. Thus, new therapies that can reverse pathological cardiac hypertrophy are highly needed.

MicroRNA (miRNA, miR), a classic type of non-coding RNA, has been shown to have a causal role in cardiovascular diseases including pathological cardiac hypertrophy and heart failure.²⁻⁴ As miRNAs can be

easily manipulated, they are promising therapeutic targets for intervention, with several on-going clinical trials. miR-92a-3p is a therapeutic target for cardiovascular disease and wound healing. MRG-110 (anti-miR-92a), a locked nucleic acid-based antisense oligonucleotide has been tested in humans for efficiency and target derepression.⁵ Besides, CDR132L, a synthetic lead-optimized oligonucleotide inhibitor of miR-132 has been tested for maladaptive remodeling (phase I study).⁶ For miRNA overexpression clinical trial, an example of miRNA delivery via nanoparticles is in the ongoing phase I clinical trial (NCT04675996) which employs a modified miR-193a-3p mimic for therapeutic intervention in oncology. miR-124 overexpression is used to treat crohn disease in the ongoing phase II clinical trial (NCT03905109). miR-30d is a miRNA whose circulating levels have been associated with response to cardiac resynchronization therapy in heart failure.⁷ Recently, we also reported that miR-30d regulated adverse cardiac remodeling by intracellular and paracrine signaling.⁸ However, if miR-30d could be a therapeutic target of pathological cardiac hypertrophy is undetermined.

In this study, we demonstrate that miR-30d suppression is a major contributor to pathological hypertrophy. Importantly, AAV9-mediated elevation of miR-30d reversed established pathological cardiac hypertrophy *in vivo*. Mechanistically, we found methyltransferase EZH2 inhibited transcription of miR-30d by promoting the methylation level of H3K27me3 in the miR-30d promoter and further identified MAP4K4 and GRP78 as target genes of miR-30d. Finally, the potential clinical relevance of miR-30d in human is underscored by the decreased serum circulating miR-30d level in chronic heart failure patients with mid-range ventricular function and the protective effects of miR-30d in human embryonic stem cell-derived cardiomyocytes hypertrophy model stimulated by PE and ISO. Therefore, our study provides the basis for pre-clinical and clinical development of miR-30d overexpression for the treatment of pathological cardiac hypertrophy and heart failure.

Methods

Ethics statement

Male C57BL/6J mice at 8-10 weeks old were purchased from Charles River (Beijing, China). The miR-30d transgenic rat were used, as we previously reported.⁸ All mice and rat were maintained in a specific pathogen-free (SPF) laboratory animal facility of Shanghai University (Shanghai, China). All procedures with animals

followed guidelines on the use and care of laboratory animals for biomedical research published by National Institutes of Health (No. 85-23, revised 1996). The present study was approved by the research ethics committee of Shanghai University (the approval number: No. ECSHU2019-013).

Cardiac hypertrophy model

The mice cardiac hypertrophy model induced by transverse aortic constriction (TAC) surgery, angiotensin II (Ang II)- and isoproterenol (ISO) infusion were performed as described previously.⁹ Mice were randomly divided into different groups. Five mice were fed in each cage.

After the mice were anaesthetized with intraperitoneal sodium pentobarbital (50 mg/kg), TAC surgery was performed by tying 7-0 silk structure to the transverse aorta with a 27-gauge needle placed parallel to that, and the transverse aorta was tied between the innominate artery and left common carotid artery after the needle was removed. Sham surgery was performed with the same surgery without tying the transverse aorta. Mice were maintained the anesthesia by mechanical ventilation using a respirator (The respiration rate should be approximately 110 per minute, with an inspiratory pressure of 17 to 18 cm H₂O.) during surgery. Body temperature was maintained at 37 ± 0.5°C during surgery.

Ang II (Sigma, USA) was infused daily by using Alzet osmotic mini-pumps (Model 2004, Alzet, USA) with a dose of 1.3 mg/kg/day for 4 weeks. The control mice were infused with saline. Mice were anaesthetized through the intraperitoneal application of sodium pentobarbital (50 mg/kg) and followed by implantation of the Ang II mini-osmotic pump.

ISO (Sigma, USA) was infused daily by using Alzet osmotic mini-pumps (Model 2002, Alzet, USA) with a dose of 30 mg/kg/day for 2 weeks. The control mice were infused with saline. Mice were anaesthetized through the intraperitoneal application of sodium pentobarbital (50 mg/kg) and followed by implantation of the ISO mini-osmotic pump.

The rat cardiac hypertrophy model was established by ISO injection. 8 weeks old male miR-30d transgenic (TG) Sprague-Dawley (SD) rat and wild type (WT) littermates were used. ISO (Sigma, USA) was intraperitoneally injected of 1.5 mg/kg/day for 14 consecutive days. The control rat were injected with saline. Rat were randomly divided into different groups.

At the end of the experiments, mice or rat were sacrificed via intraperitoneal sodium pentobarbital (60 mg/kg) and cardiac tissues were analyzed.

Adeno-associated virus (AAV) serotype 9 packaging and AAV9 treatment

HEK293T cells were cultured in a 10 cm cell culture dish and cultured with DMEM (10% fetal bovine serum

and 1% penic; zillin/streptomycin). Then cells were transfected with 10 µg of miR-30d overexpression plasmid (or control plasmid), 10 µg pAAV 2/9 (Addgene #112865) and 10 µg pAd Delta F6 (Addgene #112867) by using 100 µl Polyethylenimine (PEI) (1 mg/ml, Kingmorn, #KE1098). The supernatant and cells were collected after 48 h. AAV9 virus from the supernatant was obtained by PEG8000 precipitation. Virus from cells were obtained by the repetitive freeze thaw method. After incubated with 1 M MgCl₂ and Benzonase[®] nuclease (EMD Millipore Core, USA), AAV9 virus were purified by density gradient centrifugation with iodixanol (sigma, USA). Then the purified AAV9 virus was concentrated with concentration tube (Amicon[®] Ultra-15, Millipore, Ireland). To detect the titer of virus, viral genomic DNA was extracted by TIANamp Genomic DNA Kit (TIANGEN, China). qRT-PCR was performed to analyze the titer of virus with a standard curve. A single tail vein injection of AAV9 virus was performed at the dose of 10¹² GC per mice. According to the mature sequence of miR-30d (UGUAAA-CAUCCCCGACUGGAAG), the following sequences were designed to overexpress miR-30d and pENN.AAV. cTNT. plasmid (Addgene viral prep # 105543-AAV9) was used.

F: 5'-GATCTGTAAACATCCCCGACTGGAAG
CTCGAGCTTCCAGTCGGGGAT
GTTTACATTTTG-3',
R: 5'-AATTCAAAAATGTAAACATCCCCGACTGGAAG
CTCGAGCTTCCAGTC
GGGGATGTTTACA-3'.

Neonatal rat cardiomyocytes (NRCMs) isolation, culture and treatment

Primary neonatal rat cardiomyocytes (NRCMs) were isolated from 1 to 3-day old SD rats and purified by Percoll (Sigma, USA) gradient centrifugation, as previously described.¹⁰ In brief, hearts were isolated and cut into small pieces in ADS saline solution. The tissue was digested with trypsin (ThermoFisher, USA) and type II collagenase (Gibco, USA). After neutralization and centrifugation, separated cells were resuspended in DMEM supplemented with 10% FBS and 1% penicillin-streptomycin. Cardiac fibroblasts were discarded by using differential time adherent method. And cardiomyocytes were purified by density gradient centrifugation in Percoll solution (GE Healthcare, USA). Purified cardiomyocytes were incubated in gelatin-coated tissue culture dishes with DMEM medium mixed with 10% FBS, 5% HS, maintained in 5% CO₂ at 37°C.

To establish cardiac hypertrophy, NRCMs were treated with Ang II (1 µM, sigma, USA) or phenylephrine (PE) (100 µM, Tocris Bioscience, UK) for 48 h after starvation with serum-free DMEM (Gibco, USA) for

6–8 h. NRCM transfection was performed with Lipofectamine 2000 Reagent (Invitrogen, USA). The transfection dosages of mimic negative control (RiboBio, China) and miR-30d mimic (RiboBio, China) were 50 nM, while inhibitor negative control (RiboBio, China) and miR-30d inhibitor (RiboBio, China) were 100 nM. The transfection dosage of siRNAs for MAP4K4, GRP78 and EZH2 were 100 nM and the sequences were listed in Table S1. After transfection, the cardiac hypertrophy model was induced by PE or Ang II.

Plasmid and cell transfection

AC16 cells were cultured in Dulbecco's modified Eagle's medium (DMEM) containing 10% fetal bovine serum at 37 °C with 5% CO₂. EZH2 overexpression plasmid was purchased from vigenebio (CH882009, China). The sh-EZH2 plasmid was constructed in PLKO.TRC, and the sequences were listed in Table S2. Plasmid transfection was performed with Lipofectamine 2000 Reagent (Invitrogen, USA).

Immunofluorescence

To evaluate the size of cardiomyocytes, α -actinin staining was performed. After fixed by 4% paraformaldehyde, permeabilized with 0.5% Triton X-100, blocked with 5% BSA in PBST, cardiomyocytes were incubated with α -actinin primary antibody (sigma#A7811, 1:100) overnight at 4 °C. Then secondary antibody Cy3-AffiniPure Rabbit Anti-Mouse IgG (H+L) (1:500, Jackson ImmunoResearch Inc) was used to visualization of primary antibody. Nuclear staining was performed with DAPI. Images were captured by fluorescence microscope (Leica, German) and the size of cardiomyocytes was measured by Image J.

Wheat germ agglutinin (WGA) staining

O.C.T Compound (optimal cutting temperature compound, Sakura) embedded frozen sections of the heart samples were used for WGA staining. The 10- μ m heart cross-sections were reheated at room temperature for 20 min. Then heart cross-sections were gently washed with PBS 3 times for 5 min each, fixed with 4% paraformaldehyde for 15 min. The tissue sections were incubated with WGA working solution (Invitrogen #W11261, 1:100) for 2 h at room temperature and were stained with DAPI mounting media for 20 min in dark. Then the tissue sections were washed with PBS 3 times and sealed with 50% glycerin. Images were captured by fluorescent microscope (Leica, German), the area of cardiomyocytes was measured by Image J (NIH, USA), and a minimum of 400 cardiomyocytes per mouse was analyzed.

Hematoxylin-eosin (HE) staining

To assess the morphological changes and size of the heart, the heart samples were fixed overnight in 4% paraformaldehyde (PFA). All samples were paraffin-embedded and sectioned. HE staining was completed using a Hematoxylin and Eosin Staining Kit (Keygen, China). The image was taken under an optical microscope (Leica, Germany) at 400 \times magnification for analysis. At least 50 views and more than 400 cardiomyocytes per mouse were quantified for analysis by using Image J software (NIH, USA).

Masson's trichrome staining

To evaluate the fibrosis level of the heart, heart sections were fixed in 4% paraformaldehyde (PFA) and cut into 5 μ m sections. All sections were stained with Masson's trichrome Kit (Keygen, China) to visualize fibrotic tissue. Images were taken by Leica optical microscope (Leica, German) at 200 \times magnification for analysis. The result was obtained by using Image J software (NIH, USA) to calculate the ratio of blue (fibrotic) to the total myocardial area (health). And at least 50 views were used for analysis per mouse.

Quantitative real-time polymerase chain reaction (qRT-PCR)

Total RNA was extracted from heart tissue and cardiomyocytes by using RNAiso Plus reagent (Takara, Japan) according to the manufacturer's instructions. For miRNA analysis, the expression of miRNA was determined by using stem-loop RT method with Bulge-LoopTM miRNA qPCR Primer Set (RiboBio, China) and PCR with TB green premix Ex Taq (Takara, #RR420A) in Roche480 Detection System. 5S rRNA was used as an internal control. For mRNA analysis, cDNA was synthesized using RevertAid First Strand cDNA Synthesis Kit (ThermoFisher, USA) and was subjected to qPCR with Takara SYBR Premix Ex Taq. 18S rRNA was used as an internal control. The primer sequences used in this study were listed in Table S3. The relative expression level of gene or miRNA was calculated using the $2^{-\Delta\Delta Ct}$ method.

Western blotting

The total protein was isolated from the respective cells or tissues using protein lysis buffer with protease and phosphatase inhibitor (Keygen, #KGP250). Then the protein concentration was quantified with BCA Protein Assay Kit (Takara, #3733). Equal amounts of protein samples were separated by SDS–polyacrylamide gel electrophoresis, and then transferred to 0.2 μ m polyvinylidene fluoride (PVDF) membranes. The membranes were blocked with 5% skimmed milk for 2 h at room temperature and then incubated with primary antibodies diluted in 5% BSA (overnight at 4 °C). Primary

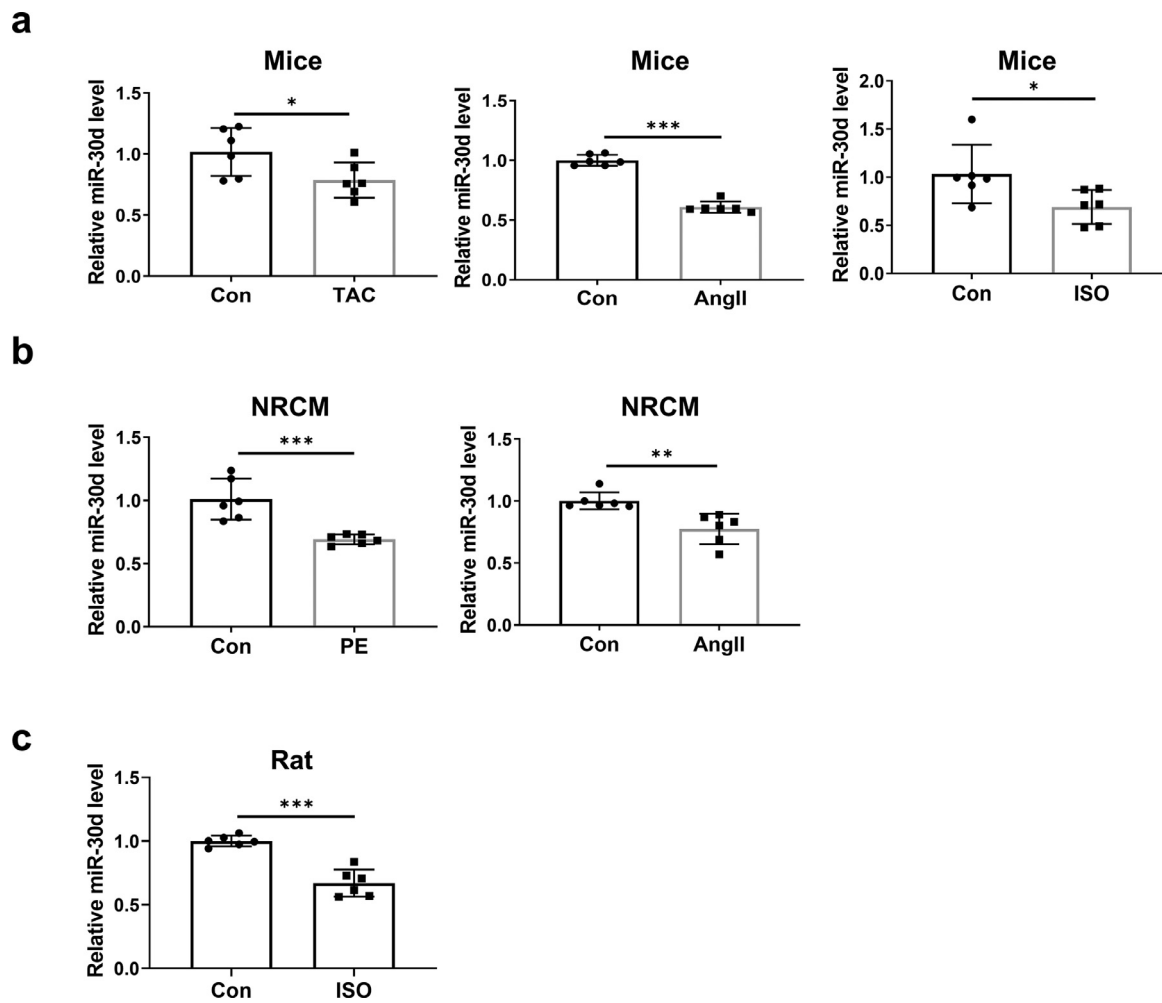


Figure 1. miR-30d is downregulated in pathological cardiac hypertrophy induced by multiple stimuli. **(a)** qRT-PCR analysis of miR-30d expression in left ventricle from mice subjected to transverse aortic constriction (TAC) surgery ($n = 6$ per group), angiotensin II (Ang II) infusion ($n = 6$ per group) and isoproterenol (ISO) infusion ($n = 6$ per group) induced cardiac hypertrophy. **(b)** qRT-PCR analysis of miR-30d expression in neonatal rat cardiomyocytes (NRCMs) treated with phenylephrine (PE, $n = 6$ per group) and angiotensin II (Ang II, $n = 6$ per group). **(c)** qRT-PCR analysis of miR-30d expression in left ventricle from rat subjected to ISO injection induced cardiac hypertrophy ($n = 6$ per group). Data are shown as means \pm SD. Statistical significance was determined by Student *t* test. *, $P < 0.05$; **, $P < 0.01$ and ***, $P < 0.001$.

antibodies that we used include: anti-GADPH (bioworld, #AP0063), anti-MAP4K4 (proteintech, #55247-1-AP), anti-GRP78 (abclonal, #A0241), anti-EZH2 (abcam, #ab191250), anti-NFATc3 (Cell Signaling Technology, #4998S). Then the membranes were incubated with the appropriate HRP-conjugated secondary antibody (1:1,0000, Jackson ImmunoResearch Inc) for 2 h at room temperature. All proteins were visualized by Tanon™ High-sig ECL Western Blotting Substrate Kit (Tanon, #180-5001) and chemical luminescence of membranes was detected by Tanon imaging system (Tanon, #5200s). The density of immunoblots was measured by Image J.

Chromatin immunoprecipitation (ChIP) assay

ChIP assay was performed as described previously.¹¹ ChIP was carried out by the ChIP Assay Kit (Millipore, USA). In brief, 10^7 AC16 cells were cross-linked with 37% formaldehyde and 1.5 M glycine. Nuclei were obtained after lysis and centrifugation. The nuclear components were extracted with nuclei lysis buffer and then obtained the DNA fragment by ultrasonic breaker (Scientz, China). The supernatant was collected, and the total volume was recorded. Then the supernatant was incubated with IgG antibody (Sigma, #SAB3700848), H3K27me3 antibody (Cell Signaling Technology, # 9733) or EZH2 antibody (abcam, #

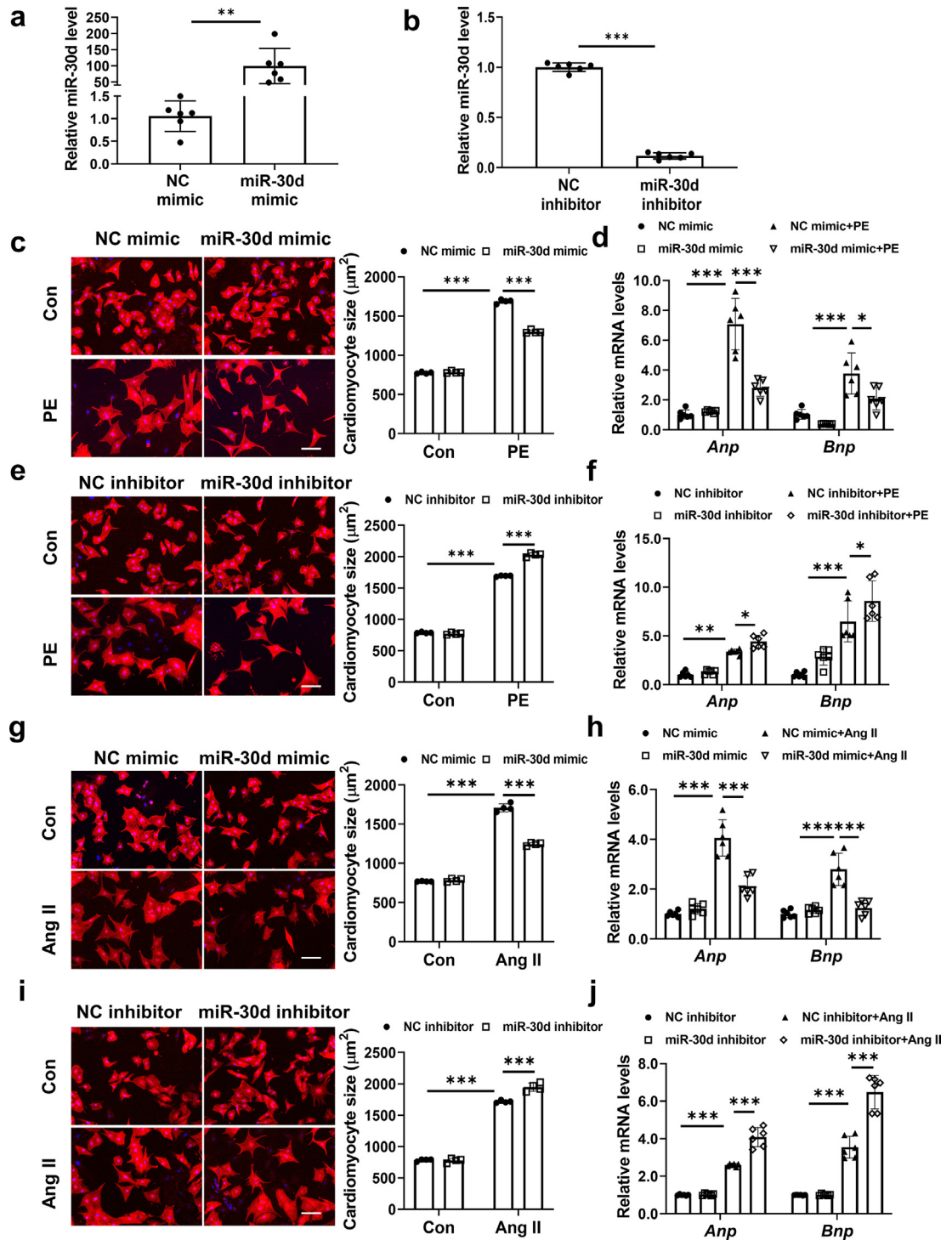


Figure 2. miR-30d protects against cardiomyocyte hypertrophy *in vitro*. (a) qRT-PCR analysis of miR-30d expression in neonatal rat cardiomyocytes (NRCM) transfected with miR-30d mimic and the corresponding negative control (NC) mimic ($n = 6$ per group). (b) qRT-PCR analysis of miR-30d expression in NRCM transfected with miR-30d inhibitor and the corresponding NC inhibitor ($n = 6$ per group). (c) **Left**, Representative immunofluorescence image of a-actinin (red)- and DAPI (blue)-stained NRCM transfected with miR-30d mimic and the NC mimic before treated with or without phenylephrine (PE) for 48 h. Scale bar, 100 μm . **Right**, Quantification of the average cell surface areas of NRCM transfected with miR-30d mimic and the NC mimic treated with or without PE. ($n = 4$ per group, number of $\text{CM} \geq 50$ cells per sample). (d) qRT-PCR analysis of hypertrophic marker gene *Anp* and *Bnp* expression in NRCM

ab3748) at 4°C overnight separately. 1% supernatant was taken as input and stored at 4°C. Then pre-cleaning G-sepharose were added into the mixture and incubated at 4°C for 90 min. After centrifugation, the supernatant was removed and beads were washed repeatedly. IP elution buffer was added to the beads and the process of de-crosslinking was performed by heating at 65°C overnight. Finally, DNA were extracted for qRT-PCR analysis. The primer sequences were as follows: Forward primer, 5'-AGCAGGCATCCATGAAATGT-3', Reverse primer, 5'-AAGTGGTTCACCAAGTGCAA-3'.

Luciferase reporter assays

For analysis the regulation between EZH2 and miR-30d, the promoter sequence of miR-30d was cloned into pGL3-basic vector. Luciferase reporter assays in A549 cell were performed as described previously.¹² For analysis the target genes of miR-30d, the sequences and mutated sequences of 3'UTR of MAP4K4 and GRP78 were cloned into pGL3-basic vector. Luciferase reporter assays in HEK293 cell and H9C2 cell were performed as described previously.¹² The sequences used in this study were listed in Table S4.

Chronic heart failure patients

All human investigations conformed to the principles outlined in the Declaration of Helsinki and were approved by the institutional review committees of Shanghai Tongji Hospital (the approval number: 2014-002). 30 chronic heart failure patients (Age: 62.4±6.4; Male:15(50%)) and 31 age- and gender-matched healthy controls (Age:62.3±4.4; Male:15(48.4%)) were enrolled. The diagnosis of chronic heart failure was diagnosis by two cardiologists according to the Heart Failure Guideline of the Chinese Society of Cardiology. All patients and healthy people were recruited with a written informed consent at Tongji Hospital (Shanghai, China)

from November 2015 to December 2016. Venous blood was collected at enrollment and was stored at -80°C until further use.

Measurement of circulating miRNAs

Measurement of circulating miRNAs was performed as described previously.¹³ In brief, total RNA in serum was isolated by using the mirVana PARIS isolation kit (Ambion, USA). *Caenorhabditis elegans* miR-39 (cel-miR-39) was added as the spike-in control. The expression of miRNA was determined by using stem-loop RT method with Bulge-Loop™ miRNA qPCR Primer Set (RiboBio, China) and PCR with TB green premix Ex Taq (Takara, #RR420A) in Roche480 Detection System. The relative expression level was calculated using the $2^{-\Delta\Delta Ct}$ method.

Human embryonic stem cells (hESCs) derived cardiomyocytes and treatment

hESCs cell line H9 were cultured in feeder-free culture conditions on Matrigel (Corning, #354230) coated plates and mTeSR medium (Stemcell, #85850). Cardiomyocytes differentiation was induced as we reported previously.¹⁴ Briefly, hESCs were seeded on matrigel-coated plates in mTeSR supplemented with 10 μM Y-27632. Differentiation was induced using CHIR99021 (Selleck, #S1263) at 6 μM for 48 h. On day 2, the medium was refreshed with the addition of Wnt-pathway inhibitor IWP2 (Selleck, #S7085) at 5 μM for 48 h. The basal medium is RPMI 1640 medium (Life Technologies, #72400047) supplemented with albumin (0.5 mg/ml) and ascorbic acid (0.2 mg/ml) from day 0 to day 8. Spontaneous beating cells start to appear at day 8, and the beating cells were cultured in RPMI 1640 supplemented with B27 for further maturation. The culture medium was changed every 2 days. After followed by a metabolic selection process to obtain a purified

transfected with miR-30d mimic and NC mimic before treated with or without PE for 48 h ($n = 6$ per group). **(e) Left**, Representative immunofluorescence image of a-actinin (red)- and DAPI (blue)-stained NRCM transfected with miR-30d inhibitor and the NC inhibitor before treated with or without phenylephrine (PE) for 48 h. Scale bar, 100 μm. **Right**, Quantification of the average cell surface areas of NRCM transfected with miR-30d inhibitor and the NC inhibitor treated with or without PE. ($n = 4$ per group, number of CM ≥ 50 cells per sample). **(f)** qRT-PCR analysis of hypertrophic marker gene Anp and Bnp expression in NRCM transfected with miR-30d inhibitor and NC inhibitor before treated with or without PE for 48 h ($n = 6$ per group). **(g) Left**, Representative immunofluorescence image of a-actinin (red)- and DAPI (blue)-stained NRCM transfected with miR-30d mimic and the NC mimic before treated with or without angiotensin II (Ang II) for 48 h. Scale bar, 100 μm. **Right**, Quantification of the average cell surface areas of NRCM transfected with miR-30d mimic and the NC mimic treated with or without Ang II. ($n = 4$ per group, number of CM ≥ 50 cells per sample). **(h)** qRT-PCR analysis of hypertrophic marker gene Anp and Bnp expression in NRCM transfected with miR-30d mimic and NC mimic before treated with or without Ang II for 48 h ($n = 6$ per group). **(i) Left**, Representative immunofluorescence image of a-actinin (red)- and DAPI (blue)-stained NRCM transfected with miR-30d inhibitor and the NC inhibitor before treated with or without Ang II for 48 h. Scale bar, 100 μm. **Right**, Quantification of the average cell surface areas of NRCM transfected with miR-30d inhibitor and the NC inhibitor treated with or without Ang II. ($n = 4$ per group, number of CM ≥ 50 cells per sample). **(j)** qRT-PCR analysis of hypertrophic marker gene Anp and Bnp expression in NRCM transfected with miR-30d inhibitor and NC inhibitor before treated with or without Ang II for 48 h ($n = 6$ per group). Data are shown as means \pm SD. Statistical significance was determined by Student t test(a-b) and two-way ANOVA test with post hoc tukey (c-j). *, $P < 0.05$; **, $P < 0.01$ and ***, $P < 0.001$.

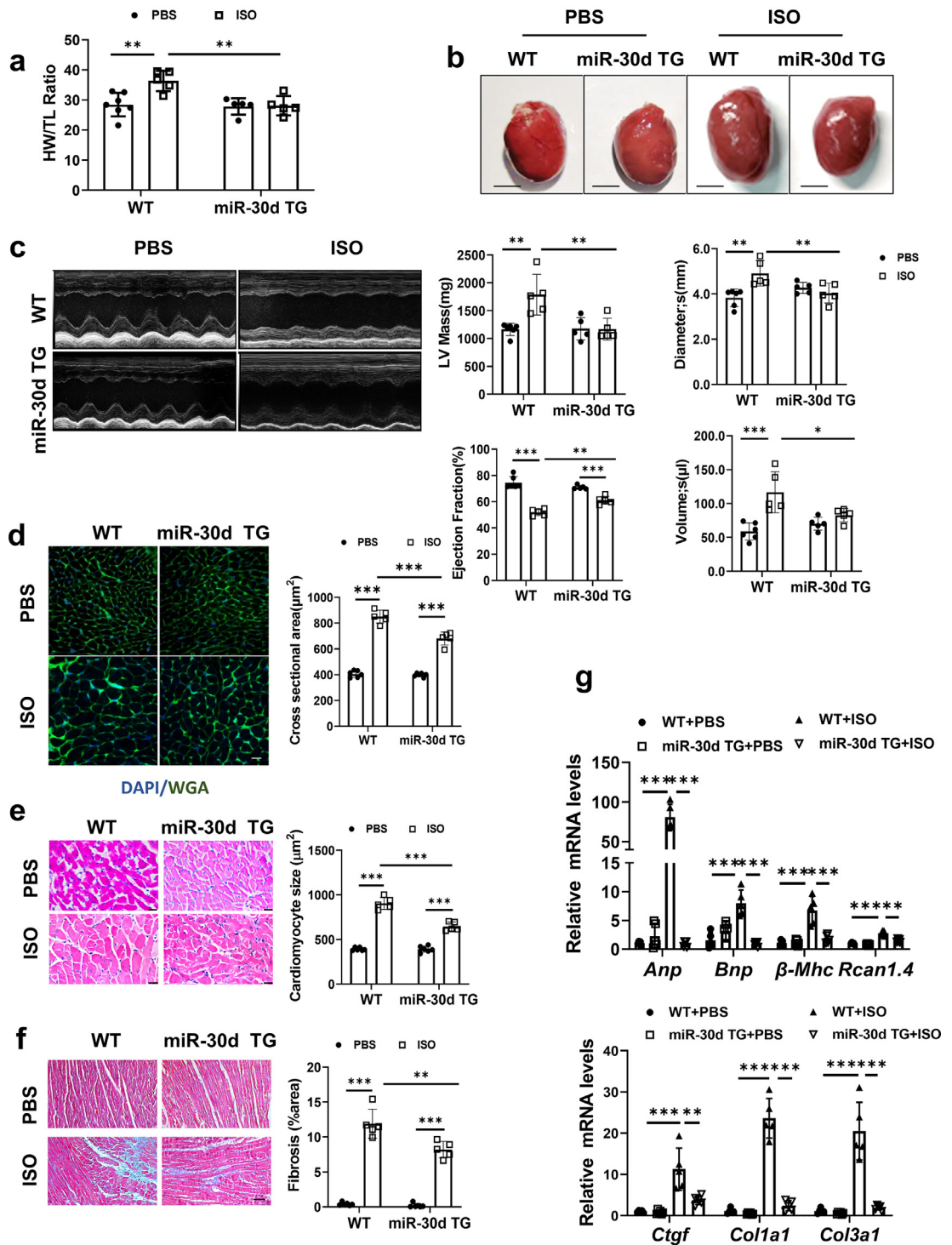


Figure 3. miR-30d prevents ISO-induced pathological cardiac hypertrophy. (a) Heart weight/tibia length (HW/TL) of miR-30d transgenic (TG) and wildtype (WT) rat injection with isoproterenol (ISO) or PBS ($n = 7,5,5,5$ per group). (b) Cardiac morphology of miR-30d TG and WT rat injection with ISO or PBS, Scale bar, 5 mm. (c) Representative echocardiographic images, echocardiographic analysis of cardiac dimensions and function of miR-30d TG and WT rat injection with ISO or PBS ($n = 5$ per group). (d) Wheat germ agglutinin (WGA) staining showed cardiomyocyte size of miR-30d TG and WT rat injection with ISO or PBS ($n = 5$ per group). Scale bar, 20 μ m. (e) Representative HE staining images and quantitative statistics of cardiomyocytes size of miR-30d TG and WT rat injection

population of hESC-CMs, cardiomyocytes were used after differentiation for 30 days.^{15,16}

Cardiomyocytes were transfected with 50 nM miR-30d mimic, 100 nM miR-30d inhibitor, 100 nM siRNA of MAP4K4 and GRP78, and corresponding negative control with lipofectamine 2000 Regent (Invitrogen, USA). After 24 h, the transfected cells were further treated with phenylephrine (PE, Tocris Bioscience, UK) and Isoproterenol (ISO, Sigma, USA). The PE and ISO were added in culture medium at 100 μ M for 48 h, and the plates were covered with aluminium foil during the treatment.

Statistical analysis

All data were analyzed by SPSS 20.0 and presented as mean \pm SD. using GraphPad Prism 8.0. An unpaired, two-tailed Student's *t*-test was used for comparisons

between two groups. Two-way ANOVA with post hoc tukey was performed to compare multiple groups. Differences were considered significant with $P < 0.05$. The area under the curve (AUC) to assessing the diagnostic value of circulating miR-30d level by using a receiver operator characteristic (ROC) curve and statistical analysis was performed using MedCalc (MedCalc Software, Belgium). Differences were considered significant with $p < 0.05$.

RRID tags

The cell lines have STR authentication and mycoplasma testing. The cell identification report and antibody product datasheets have been provided in the Supplemental Data.

Reagent or resource	Source	Identifier	RRID
Antibodies			
EZH2	Abcam	ab3748	AB_304045
H3K27me3	Cell Signaling Technology	9733	AB_2616029
GAPDH	Bioworld	AP0063	AB_2651132
MAP4K4	Proteintech	55247-1-AP	AB_10836939
GRP78	Abclonal	A0241	AB_2757054
NFATc3	Cell Signaling Technology	49985	AB_2152771
Cell lines			
AC16	Millipore	SCC109	CVCL_4U18
H9	Millipore	SCC109	CVCL_9773
Chemicals, peptides, and recombinant proteins			
angiotensin II (Ang II)	Sigma	A9525	
phenylephrine (PE)	Tocris Bioscience	61-76-7	
isoproterenol (ISO)	Sigma	51-30-9	
WGA (wheat germ agglutinin)	Sigma	L4895	
Critical commercial assays			
Western Blot lysis buffer	KeyGEN	Western Blot lysis buffer	
Masson's trichrome staining Kit	KeyGEN	KGMST-8003	
H&E staining Kit	KeyGEN	KGA224	
ChIP Assay Kit	Millipore	17-295	
Software and algorithms			
ImageJ Software	NIH	N/A	
SPSS20.0		N/A	
GraphPad Prism 8.0	GraphPad	N/A	
MedCalc	MedCalc	N/A	

with ISO or PBS ($n = 5$ per group). Scale bar, 40 μ m. (f) Representative images of Masson's trichrome stained, and quantification of fibrosis area (%) showed a significant decrease of fibrosis areas in miR-30d TG injection with ISO compared to WT rat injection with ISO or PBS ($n = 5$ per group). Scale bar, 25 μ m. (g) qRT-PCR analysis for the mRNA levels of hypertrophic markers (Anp, Bnp, β -Mhc, and Rcan1.4) and the fibrotic markers (Col1a1, Col3a1, and Ctgf) in miR-30d TG and WT rat injection with ISO or PBS ($n = 5$ per group). Data are presented as mean \pm SD. Statistical significance was determined two-way ANOVA with post hoc tukey. *, $P < 0.05$; **, $P < 0.01$ and ***, $P < 0.001$.

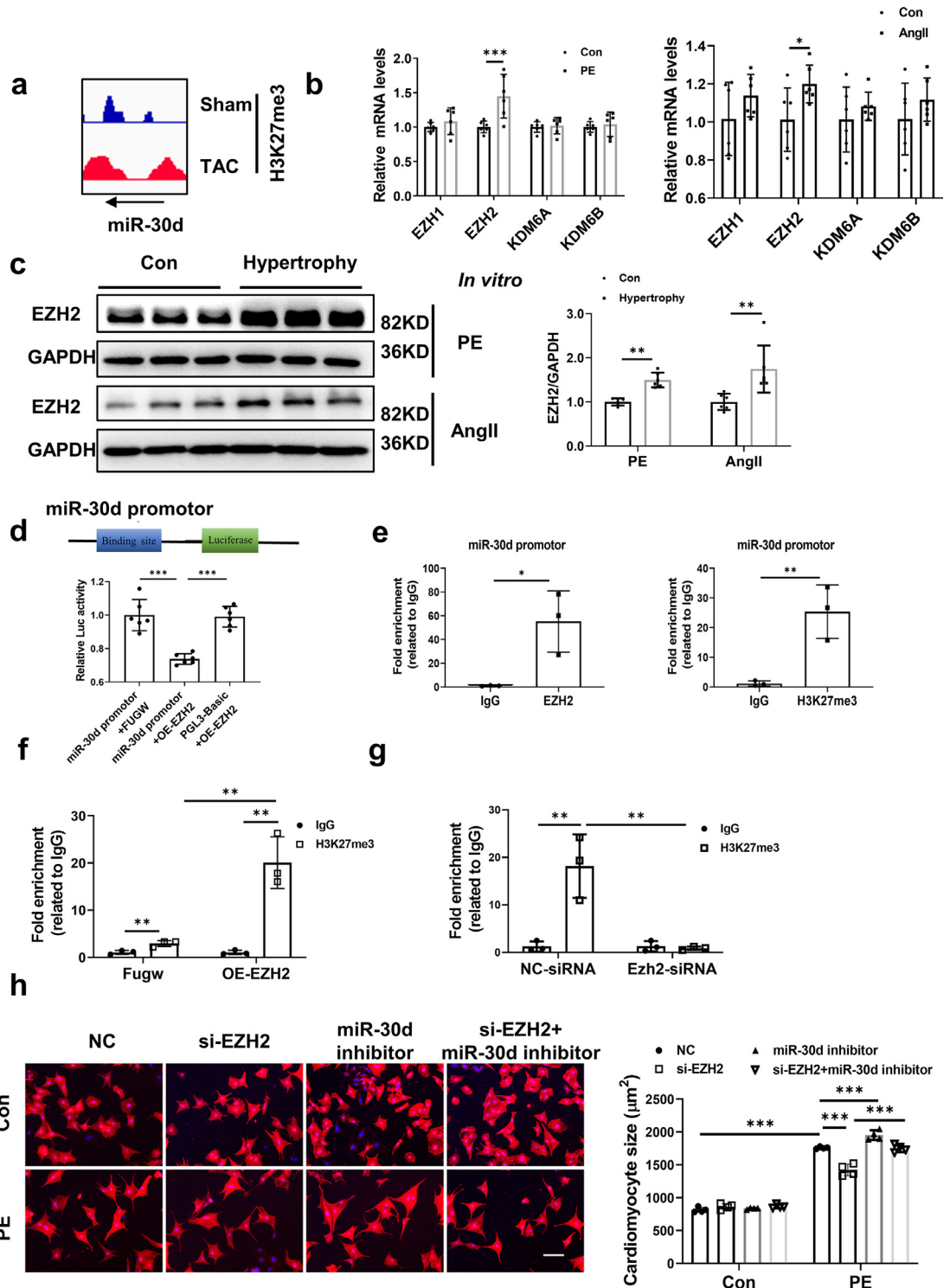


Figure 4. EZH2 regulates H3K27me3 enrichment on the miR-30d promoter. (a) Genomic views of the H3K27me3 modification of miR-30d related to transverse aortic constriction (TAC) induced cardiac hypertrophy (GSE93752). (b) qRT-PCR analysis of the expression of H3K27 methyltransferase (EZH1 and EZH2) and demethylase (KDM6A and KDM6B) mRNA in neonatal rat cardiomyocytes (NRCMs) treated with phenylephrine (PE, $n=6$ per group) and angiotensin II (Ang II, $n=6$ per group). (c) Western blot analysis of the expression of EZH2 protein level in NRCMs treated with PE ($n=6$ per group) and Ang II ($n=6$ per group). (d) Dual-luciferase reporter assay showed the regulation between EZH2 and miR-30d in AC16 ($n=6$ per group). (e) ChIP assay was performed to detect EZH2

Role of funding source

The Funders do not play any roles in study design, data collection, data analyses, interpretation, or writing of report.

Results

miR-30d is downregulated in pathological cardiac hypertrophy induced by multiple stimuli

To investigate the role of miR-30d in pathological cardiac hypertrophy, we determined the expression of miR-30d in different murine models of pathological cardiac hypertrophy. miR-30d was found to be consistently decreased in mouse hypertrophic hearts induced by TAC surgery, Ang II perfusion and ISO perfusion (Figure 1a). In parallel, miR-30d was significantly reduced in NRCMs treated with PE or Ang II (Figure 1b). Finally, miR-30d expression was decreased in ISO induced rat hypertrophic heart (Figure 1c). Collectively, these data suggest that miR-30d knockdown might be a major mediator of pathological cardiac hypertrophy.

miR-30d overexpression is anti-hypertrophy both in vitro and in vivo

To investigate if miR-30d is functionally involved in the development of cardiac hypertrophy, cellular models of cardiomyocyte hypertrophy induced by PE or Ang II in NRCMs were treated with miR-30d mimic and miR-30d inhibitor (Figure 2a and b). In PE-induced cardiac hypertrophy model, overexpression of miR-30d could attenuate PE-induced increase in cardiomyocytes size and inhibit the elevation of *Anp* and *Bnp* (Figure 2c and d). On the other hand, inhibition of miR-30d had a further deleterious effect on PE-induced cardiac hypertrophy based on the analysis of cardiomyocytes size and the expression levels of *Anp* and *Bnp* (Figure 2e and f). Consistently, Ang II-induced cardiomyocyte hypertrophy was significantly suppressed by miR-30d overexpression but markedly exacerbated by miR-30d inhibition as determined by cardiomyocytes size and the expression levels of *Anp* and *Bnp* (Figure 2g-j). Moreover, miR-30d TG rat was found to be protective for ISO-induced hypertrophy as evidenced by decreased heart weight to tibial length ratio, improved cardiac

function parameters (left ventricular volume and ejection fraction), decreased cardiomyocyte size and cardiac fibrosis level (Figure 3, Table S5). Collectively, these data suggest a functional role of miR-30d in cardiomyocyte hypertrophy.

Low expression of miR-30d in pathological cardiac hypertrophy is mediated by EZH2-dependent H3K27me3 modification in miR-30d promotor

To investigate the potential mechanism responsible for the downregulation of miR-30d in cardiac hypertrophy, we analyzed the promotor of miR-30d in TAC induced cardiac hypertrophy. Interestingly, the H3K27me3 intensity was significantly increased in miR-30d promotor in TAC induced cardiac hypertrophy (Figure 4a). Then we further analyzed the expression of H3K27 methyltransferase (EZH1 and EZH2) and demethylase (KDM6A and KDM6B) in hypertrophic cardiomyocytes. Using qRT-PCR, we found that EZH2 was increased in hypertrophic cardiomyocytes induced by PE and Ang II (Figure 4b). Moreover, by western blotting, we also found that EZH2 was increased in hypertrophic models both *in vitro* and *in vivo* (Figure 4c and Figure S1a). We further confirmed that EZH2 negatively regulated miR-30d levels in cardiomyocytes (Figure 4d and Figure S1b-e).

To gain further insights on miR-30d downregulation via H3K27 modifiers by EZH2, chromatin immunoprecipitation (ChIP) assay was performed in AC16 cells using antibodies against EZH2 and H3K27me3. It was found that EZH2 could bind to miR-30d promotor region (Figure 4e). EZH2 overexpression promoted H3K27me3 enrichment in the miR-30d promotor region (Figure 4f), while EZH2 knockdown suppressed H3K27me3 levels (Figure 4g). Collectively, these results indicate that EZH2 directly regulates miR-30d expression in cardiomyocytes by modulating the status of H3K27me3 at the miR-30d promotor.

To further investigate if EZH2 regulated cardiac hypertrophy mediated by miR-30d, we silenced both EZH2 and miR-30d in cardiomyocytes under PE and Ang II stimulated. Knockdown EZH2 could reduce the cardiomyocyte size, while inhibition of miR-30d could reverse that (Figure 4h and Figure S1f). These data

binding and H3K27me3 enrichment on the miR-30d promotor region in AC16 ($n = 3$ per group). (f) ChIP assay was performed to detect H3K27me3 level enrichment on the miR-30d promotor region when AC16 was treated with EZH2 overexpression plasmid (OE) or negative control Fugw plasmid for 48 h ($n = 3$ per group). (g) ChIP assay was performed to detect H3K27me3 level enrichment on the miR-30d promotor region when AC16 was treated with EZH2 siRNA or control siRNA ($n = 3$ per group). (h) **Left**, Representative immunofluorescence image of a-actinin (red)- and DAPI (blue)-stained NRCM transfected with miR-30d inhibitor and EZH2 siRNA before treated with or without PE for 48 h. Scale bar, 100 μ m. **Right**, Quantification of the average cell surface areas of NRCM transfected with miR-30d inhibitor and EZH2 siRNA before treated with or without PE. ($n = 4$ per group, number of CM ≥ 50 cells per sample). Data are presented as mean \pm SD. Statistical significance was determined by Student t test (b-c, e) and two-way ANOVA test with post hoc tukey (d, f-h). *, $P < 0.05$; **, $P < 0.01$ and ***, $P < 0.001$.

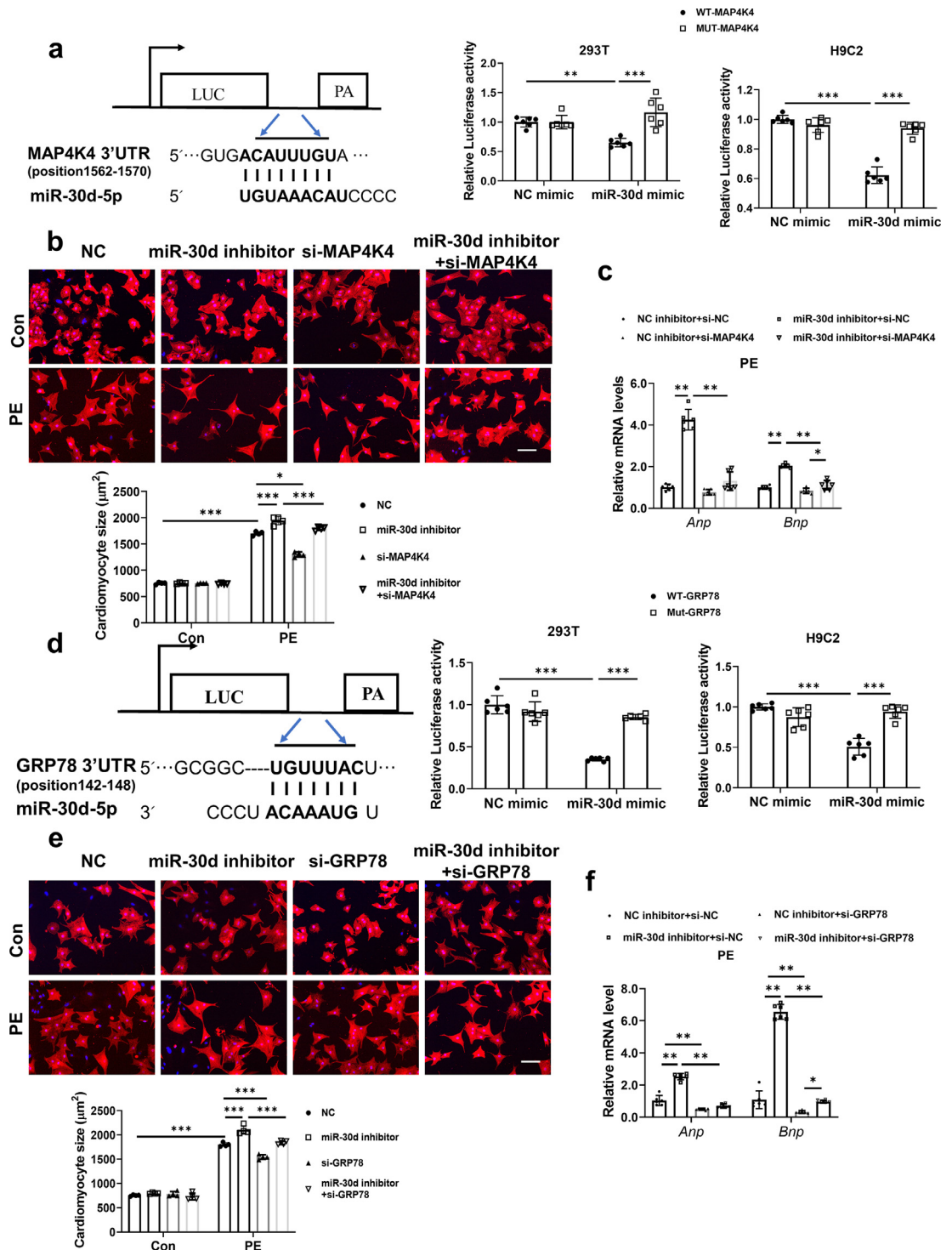


Figure 5. miR-30d directly targets MAP4K4 and GRP78. (a) Luciferase reporter assay showed that miR-30d could target to the 3'UTR region of MAP4K4 in H9C2 and 293T cells ($n = 6$ per group). (b) **Left**, Representative immunofluorescence image of α -actinin (red)- and DAPI (blue)-stained neonatal rat cardiomyocytes (NRCM) transfected with miR-30d inhibitor and MAP4K4 siRNA before treated with or without phenylephrine (PE) for 48 h. Scale bar, 100 μm . **Right**, Quantification of the average cell surface areas of NRCM transfected with miR-30d inhibitor and MAP4K4 siRNA before treated with or without PE. ($n = 4$ per group, number of $\text{CM} \geq 50$ cells per sample). (c) qRT-PCR analysis of hypertrophic marker gene *Anp* and *Bnp* expression in PE-treated NRCM transfected with miR-30d

suggest that the regulation of EZH2 in cardiac hypertrophy is mediated by miR-30d.

miR-30d directly targets MAP4K4 and GRP78

MAP4K4 is a target gene of miR-30d that we have previously reported in mediating cardiomyocyte apoptosis.⁷ However, if MAP4K4 is also a functional target of miR-30d in its effects on regulating pathological cardiac hypertrophy remains unclear. We first showed that miR-30d negatively regulated the expression of MAP4K4 by binding to the 3'UTR in cardiomyocytes (Figure 5a and Figure S2a-d). The protein levels of MAP4K4 were upregulated in *in vivo* (Ang II, TAC and ISO induced cardiac hypertrophy) and *in vitro* (Ang II and PE induced cardiomyocyte hypertrophy) hypertrophic models (Figure S2e), which is consistent with the fact that miR-30d was repressed in hypertrophic models *in vivo* and *in vitro*. Moreover, MAP4K4 was downregulated in the heart of miR-30d TG rat (Figure S2f). In addition, MAP4K4 inhibition could attenuate the pro-hypertrophic effects of miR-30d inhibitor in PE and Ang II induced hypertrophic model as determined by cardiomyocytes size and the expression levels of Anp and Bnp (Figure 5b and c, Figure S3). Collectively, these data suggest that MAP4K4 at least partly mediates the effects of miR-30d in regulating cardiomyocyte hypertrophy.

GRP78 (Glucose-Regulated Protein of 78 kDa) is a reported target of miR-30d in cancer¹⁷ and has been reported to promote cardiac hypertrophy.¹⁸ Therefore, we attempted to explore whether GRP78 is a functional target gene of miR-30d in mediating cardiac hypertrophy. By luciferase reporter assays, we showed that miR-30d reduced the luciferase activity in H9C2 cells and 293T cells, but have no effect in mutated forms of the 3'UTR of miR-30d (Figure 5d), suggesting GRP78 is a direct target gene of miR-30d. Moreover, miR-30d could negatively regulate the expression of GRP78 (Figure S4a-d). We also found that GRP78 was increased in cellular and animal models of hypertrophy, and decreased in miR-30d TG rat (Figure S4e and f). Finally, GRP78 inhibition could attenuate the pro-hypertrophic effects of miR-30d inhibitor in PE and Ang II induced hypertrophic model (Figure 5e and f, Figure S5). These data suggest that GRP78 is another target gene of miR-30d, at least partly mediating cardiomyocytes hypertrophy.

MAP4K4 and GRP78 control NFAT signaling

To further explore how MAP4K4 and GRP78 regulate cardiac hypertrophy, we investigated whether MAP4K4 and GRP78 could regulate each other. qRT-PCR and western blot analysis showed that MAP4K4 and GRP78 could not regulate each other in cardiomyocytes (Figure 6a–d), suggesting that MAP4K4 and GRP78 regulate cardiac hypertrophy independently.

As calcineurin-NFAT signaling serves a regulatory role in maladaptive hypertrophy and heart failure,^{19–21} we investigated if MAP4K4 and GRP78 regulated cardiac hypertrophy via calcineurin-NFAT signaling in cardiomyocytes. Knockdown of MAP4K4 or GRP78 could repress NFATc3 at the protein level in cardiomyocytes (Figure 6e and f), in parallel with miR-30d overexpression *in vitro* and *in vivo* (Figure 6g and h). Finally, NFATc3 was increased by miR-30d inhibition (Figure 6i). These data demonstrate that MAP4K4 and GRP78 promote calcineurin-NFAT signaling in cardiomyocytes.

Therapeutic overexpression of miR-30d reverses established pathological cardiac hypertrophy

As we have demonstrated the functional role of miR-30d in pathological cardiac hypertrophy, we investigated the therapeutic effects of miR-30d in an established pathological cardiac hypertrophy model. Two weeks after the induction of cardiac hypertrophy by TAC surgery, mice were injected with AAV9-miR-30d via tail vein injection (Figure 7a and b). Therapeutic overexpression of miR-30d by AAV9-miR-30d could reverse established pathological cardiac hypertrophy as demonstrated by the decreased heart size, improved cardiac function parameters (left ventricular volume and ejection fraction), decreased cardiomyocytes size, attenuated fibrosis level, and reduced expression levels of hypertrophic and fibrotic genes (Figure 7c–i, Table S6). In addition, therapeutic overexpression of miR-30d by AAV9-miR-30d could repress the expression of MAP4K4, GRP78 and NFATc3 (Figure S6). Taken together, our study suggests that overexpression of miR-30d reverses pathological cardiac hypertrophy and heart failure.

miR-30d is of clinical relevance in human

To confirm the clinical relevance of our findings of miR-30d in human, we firstly determined the serum level of

inhibitor and MAP4K4 siRNA. (*n* = 6 per group). (d) Luciferase reporter assay showed that miR-30d could target to the 3'UTR region of GRP78 in 293T and H9C2 cells (*n* = 6 per group). (e) **Left**, Representative immunofluorescence image of a-actinin (red)- and DAPI (blue)-stained NRCM transfected with miR-30d inhibitor and GRP78 siRNA before treated with or without PE for 48 h. Scale bar, 100 μ m. **Right**, Quantification of the average cell surface areas of NRCM transfected with miR-30d inhibitor and GRP78 siRNA before treated with or without PE. (*n* = 4 per group, number of CM \geq 50 cells per sample). (f) qRT-PCR analysis of hypertrophic marker gene Anp and Bnp expression in PE-treated NRCM transfected with miR-30d inhibitor and GRP78 siRNA. (*n* = 6 per group). Data are presented as mean \pm SD. Statistical significance was determined two-way ANOVA with post hoc tukey. *, *P* < 0.05; **, *P* < 0.01 and ***, *P* < 0.001.

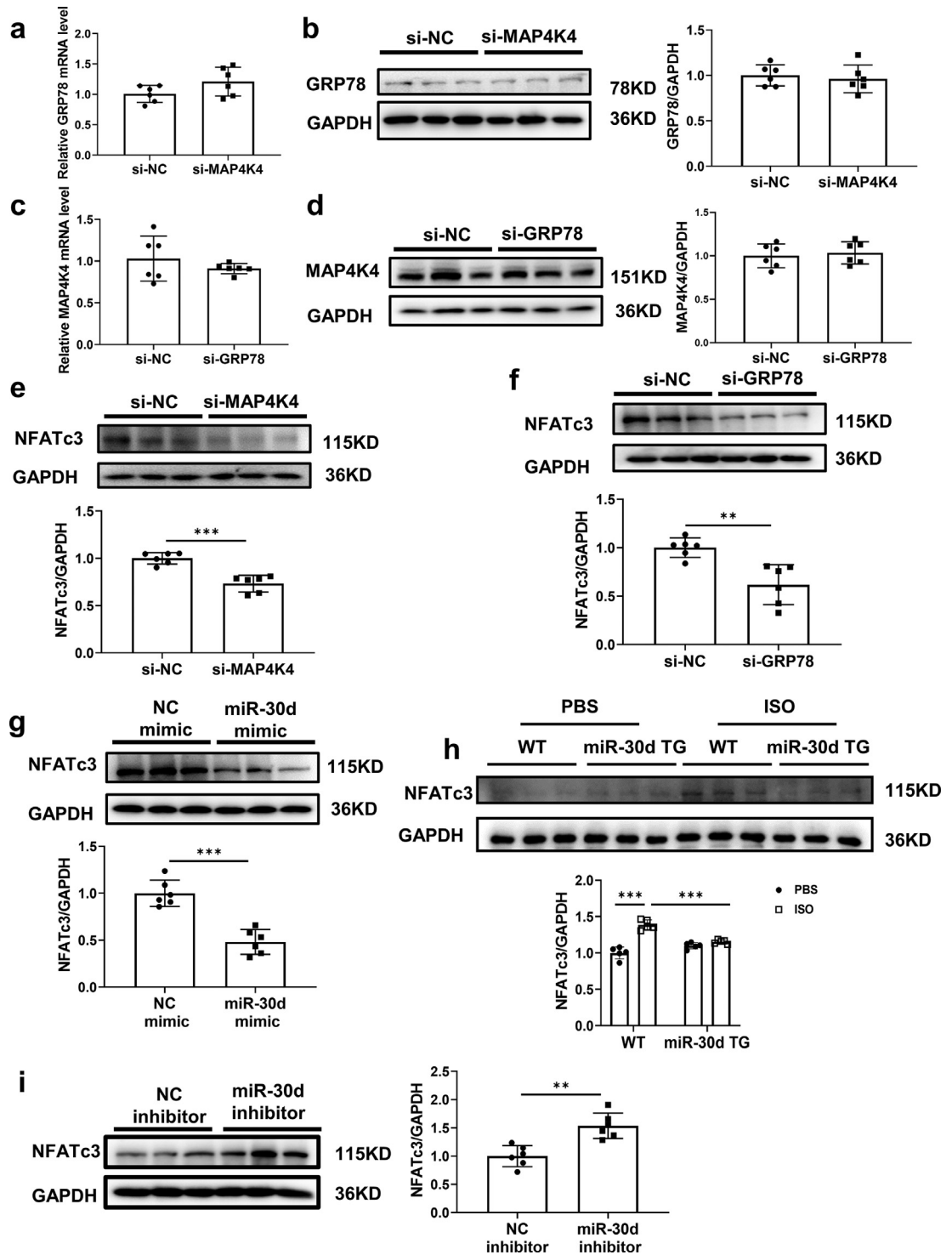


Figure 6. MAP4K4 and GRP78 control NFAT signaling. (a) qRT-PCR analysis of the expression of GRP78 mRNA level in neonatal rat cardiomyocytes (NRCM) treated with MAP4K4 siRNA or negative control (NC) siRNA for 48 h ($n = 6$ per group). (b) Western blot analysis and quantification of the expression of GRP78 protein level in NRCM treated with MAP4K4 siRNA or NC siRNA for 48 h ($n = 6$ per group). (c) qRT-PCR analysis the expression of MAP4K4 mRNA level in NRCM treated with GRP78 siRNA or NC siRNA for 48 h ($n = 6$ per group). (d) Western blot analysis and quantification of the expression of MAP4K4 protein level in NRCM treated with GRP78 siRNA or NC siRNA for 48 h ($n = 6$ per group). (e) Western blot analysis and quantification of the expression of NFATc3 protein level

miR-30d in patients with chronic heart failure and mid-range ejection fraction. A total of 30 chronic heart failure patients and 31 age- and gender-matched healthy controls were enrolled. The clinical characteristics of these chronic heart failure patients were presented in Table S7. Circulating miR-30d level was significantly decreased in chronic heart failure (Figure 8a). The receiver-operator characteristic (ROC) curve suggested that circulating miR-30d might be a biomarker for chronic heart failure with an area under the curve (AUC) of 0.906 ($P < 0.001$). Serum miR-30d predicted chronic heart failure with a specificity of 80.65% and a sensitivity of 86.67% (Figure 8b). Thus, serum miR-30d could be potentially used as a biomarker for chronic heart failure.

Besides, we established a cardiac hypertrophy model in human embryonic stem cells-derived cardiomyocytes after treatment with PE and ISO. We found that miR-30d was suppressed in hypertrophic human embryonic stem cells-derived cardiomyocytes (Figure 9a). Then, we found that miR-30d could repress hypertrophy in human embryonic stem cells-derived cardiomyocytes treated with PE and ISO, while miR-30d inhibition exacerbate that (Figure 9b). In human embryonic stem cells-derived cardiomyocytes, we also found miR-30d could negatively regulate the protein expression of MAP4K4 and GRP78 (Figure 9c and d). Moreover, either MAP4K4 or GRP78 inhibition could attenuate the prohypertrophic effects of miR-30d inhibitor in PE and ISO induced hypertrophic model in human embryonic stem cells-derived cardiomyocytes (Figure 9e). These results highlight the potential translational of miR-30d in human pathological cardiac hypertrophy and heart failure.

Discussion

Pathological cardiac hypertrophy is a major risk factor for many cardiovascular diseases. Notably, pathological cardiac hypertrophy precedes the development of overt heart failure (HF). Thus, reversing maladaptive hypertrophy is considered to be a therapeutic approach to prevent the development of heart failure. Here, we report that miR-30d plays a critical role in pathological cardiac hypertrophy. We show that miR-30d is down-regulated in pathological cardiac hypertrophy and overexpression

of miR-30d can ameliorate pathological cardiac hypertrophy. Our study provides the basis for pre-clinical and clinical development of miR-30d overexpression for the treatment of pathological cardiac hypertrophy and heart failure.

As miRNAs are emerging as promising therapeutic targets for drug development,²²⁻²⁸ we reported downregulation of miR-30d in different cardiac hypertrophy models both *in vivo* and *in vitro*, which implied that miR-30d may be a crucial molecular orchestrator and a promising therapeutic target for pathological cardiac hypertrophy. To investigate the therapeutic potential of miR-30d in the clinical situations, AAV9 expressing miR-30d was designed to treat established pathological cardiac hypertrophy. We found that miR-30d therapy could improve heart function, relieve cardiac hypertrophy and fibrosis, suggesting that miR-30d is a promising therapeutic target for pathological cardiac hypertrophy. The restoration of miR-30d could be a potential therapeutic strategy for the treatment of cardiac hypertrophy and heart failure. Besides, miR-30d is a conserved miRNA known to have oncosuppressive properties by regulating autophagy, apoptosis, proliferation, migration and invasion.²⁹⁻³¹ Considering its high evolutionary conservation, miR-30d has potential for clinical application in humans. Accordingly, we further found the protective effect of miR-30d also existed in the human embryonic stem cells-derived cardiomyocytes hypertrophy model. More importantly, the results from our small sample size cohort confirms the clinical relevance of miR-30d in humans. Consistent with our clinical finding, in our previous work, we also found that lower levels of miR-30d was associated with lower left ventricular ejection fraction (LVEF).⁸ It will be interesting to determine if circulating miR-30d could be a biomarker for patients with cardiac hypertrophy before developing HF.

Of note, miR-30d showed a different expression profile in cardiac hypertrophy in published literature. Few papers reported that miR-30d was increased, such as Morishima *et al* found miR-30d was increased in the atrium and serum of Ang II-induced cardiovascular complications in rats.³² Instead, most of the studies showed that miR-30d was down-regulated triggered by adverse cardiac remodeling, such as in heart samples of chronic kidney disease (CKD)-induced left ventricular

in NRCM treated with MAP4K4 siRNA or NC siRNA for 48 h ($n = 6$ per group). (f) Western blot analysis and quantification of the expression of NFATc3 protein level in NRCM treated with GRP78 siRNA or NC siRNA for 48 h ($n = 6$ per group). (g) Western blot analysis and quantification of the expression of NFATc3 protein level in NRCM treated with miR-30d mimic or NC mimic for 48 h ($n = 6$ per group). (h) Western blot analysis and quantification of the expression of NFATc3 protein level in miR-30d transgenic (TG) and wildtype (WT) rat injection with isoproterenol (ISO) ($n = 5$ per group). (i) Western blot analysis and quantification of the expression of NFATc3 protein level in NRCM treated with miR-30d inhibitor or NC inhibitor for 48 h ($n = 6$ per group). Data are presented as mean \pm SD. Statistical significance was determined by Student *t* test (a-g, i) and two-way ANOVA with post hoc tukey (h). **, $P < 0.01$ and ***, $P < 0.001$.

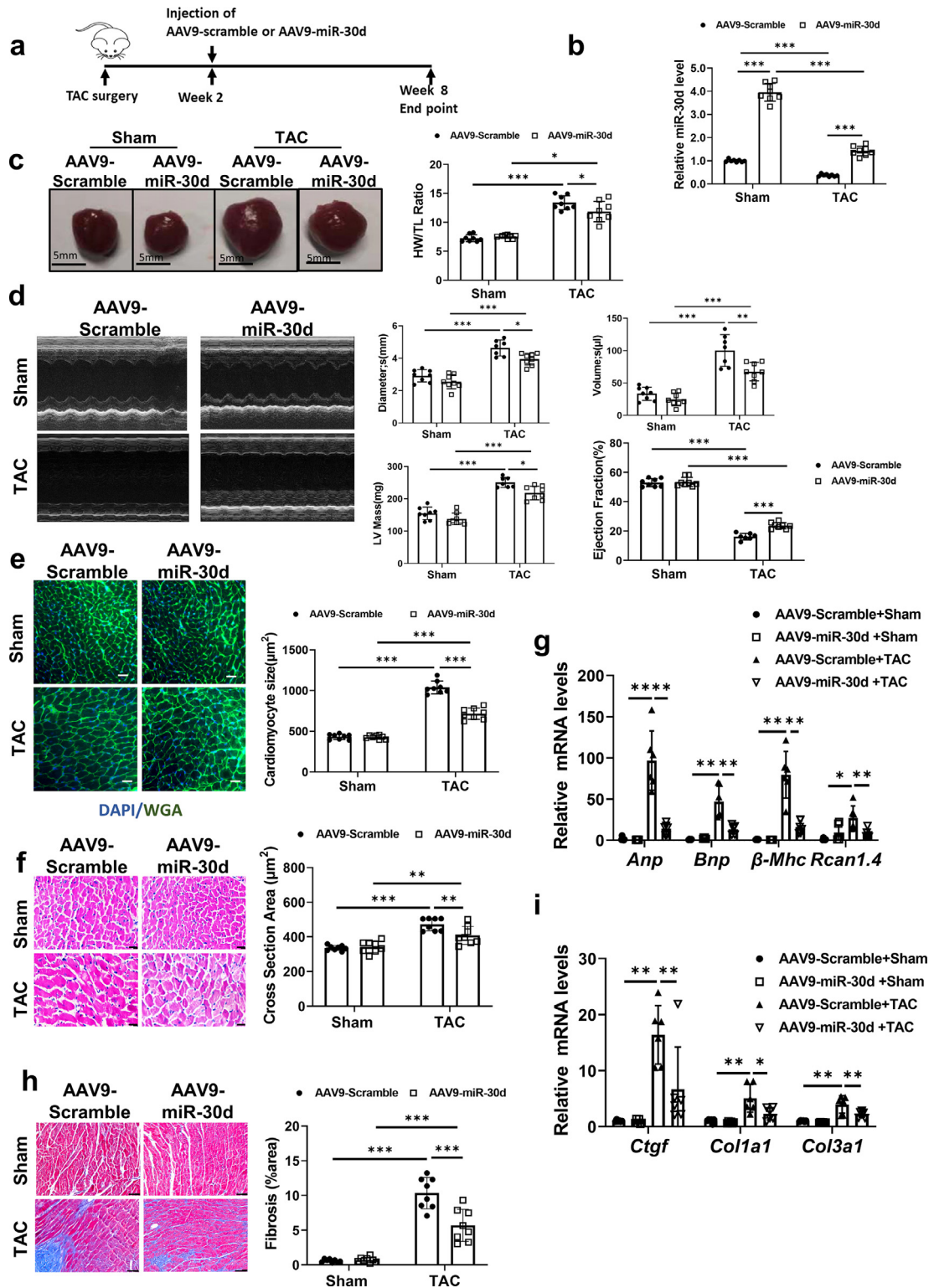


Figure 7. miR-30d therapy is effective in hypertrophic hearts. (a) Schedule time scale and experimental strategy for transverse aortic constriction (TAC) surgery, and AAV injection. (b) qRT-PCR analysis of miR-30d expression in mice injected with AAV9-miR-30d or AAV9-scramble at 2 wk after the sham or TAC surgery ($n = 8$ per group). (c) Cardiac morphology and heart weight/tibia length (HW/TL) ratio in mice injected with AAV9-miR-30d or AAV9-scramble at 2 wk after the Sham or TAC surgery ($n = 8$ per group, Scale bar, 5 mm). (d)

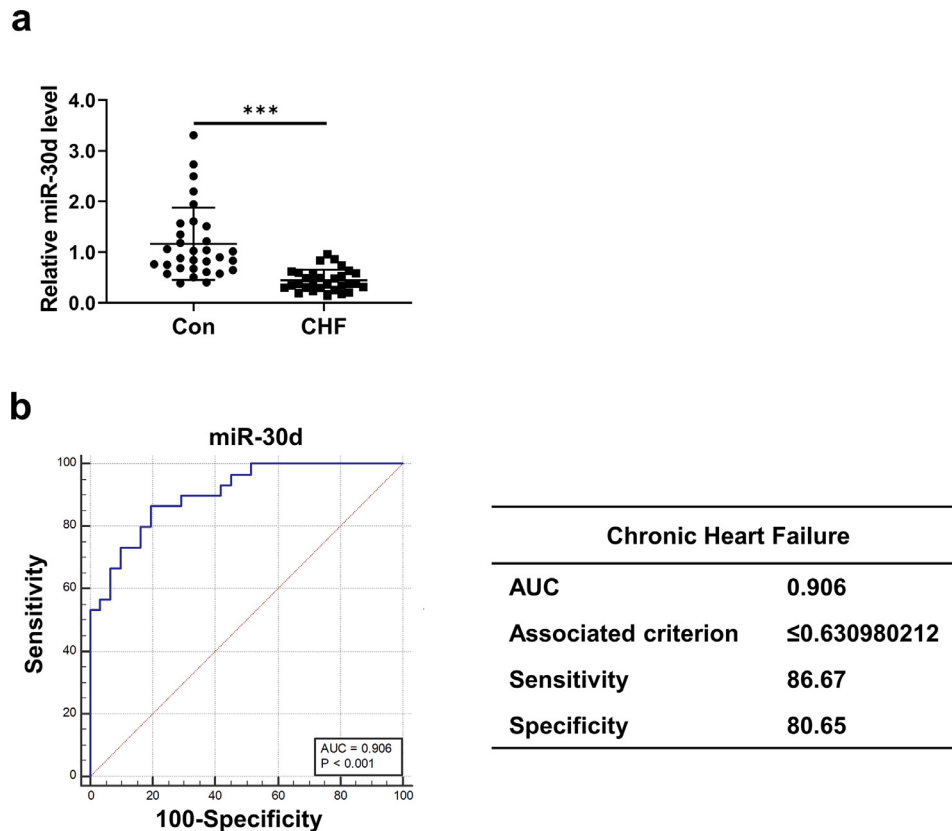


Figure 8. miR-30d is of clinical relevance in human. **(a)** qRT-PCR analysis of the expression of miR-30d level in human serum from chronic heart failure and healthy controls ($n = 31$ in healthy controls, 30 in chronic heart failure). **(b)** The receiver-operator characteristic (ROC) curves for distinguishing the diagnostic value of circulating miR-30d level in chronic heart failure patients. Data are presented as mean \pm SD. Statistical significance was determined by Student t test (a). ***, $P < 0.001$.

hypertrophy (LVH) mice model and in serum samples of dogs with eccentric or concentric cardiac hypertrophy induced by myxomatous mitral valve degeneration (MMVD) or pulmonic stenosis (PS).^{33,34} Moreover, the *in vivo* role of miR-30d in cardiac remodeling was explored in some studies. We and Bao et al. both showed that miR-30d was down-regulated in cardiac hypertrophy and pointed out that miR-30d could ameliorate hypertrophy *in vivo*.³³ The degree of cardiac hypertrophy may be the key determinant of miR-30d in

different models, as proposed in our previous study. Which is, miR-30d was increased in adaptive response, while was decreased in maladaptive response.⁷ In addition, another study showed marked activation of miR-30d in diabetic heart, which was associated with increased caspase-1 and pyroptosis.³⁵ The different changes and functions of miR-30d in diabetic heart may be due to the reasons as follows. First, the stimulation of adverse cardiac remodeling induced by ISO, ang II and TAC used in our study was totally different from

Representative echocardiographic images, cardiac function parameters of mice injected with AAV9-miR-30d or AAV9-scramble at 2 wk after the sham or TAC surgery ($n = 8$ per group). **(e)** Wheat germ agglutinin (WGA) staining showed cardiomyocyte size of mice injected with AAV9-miR-30d or AAV9-scramble at 2 wk after the sham or TAC surgery ($n = 8$ per group). Scale bar, 20 μ m. **(f)** Representative HE staining images and quantitative statistics of cardiomyocytes size of mice injected with AAV9-miR-30d or AAV9-scramble at 2 wk after the sham or TAC surgery ($n = 8$ per group). Scale bar, 40 μ m. **(g)** qRT-PCR analysis for the mRNA levels of hypertrophic markers (Anp, Bnp, β -Mhc, and Rcan1.4) in mice injected with AAV9-miR-30d or AAV9-scramble at 2 wk after the sham or TAC surgery ($n = 8$ per group). **(h)** Representative images of Masson's trichrome stained, and quantification of fibrosis area (%) in mice injected with AAV9-miR-30d or AAV9-scramble at 2 wk after the sham or TAC surgery ($n = 8$ per group), Scale bar, 25 μ m. **(i)** qRT-PCR analysis for the mRNA levels of fibrotic markers (Col1a1, Col3a1, and Ctgf) in mice injected with AAV9-miR-30d or AAV9-scramble at 2 wk after the sham or TAC surgery ($n = 8$ per group). Data are presented as mean \pm SD. Statistical significance was determined by two-way ANOVA with post hoc tukey. *, $P < 0.05$; **, $P < 0.01$ and ***, $P < 0.001$.

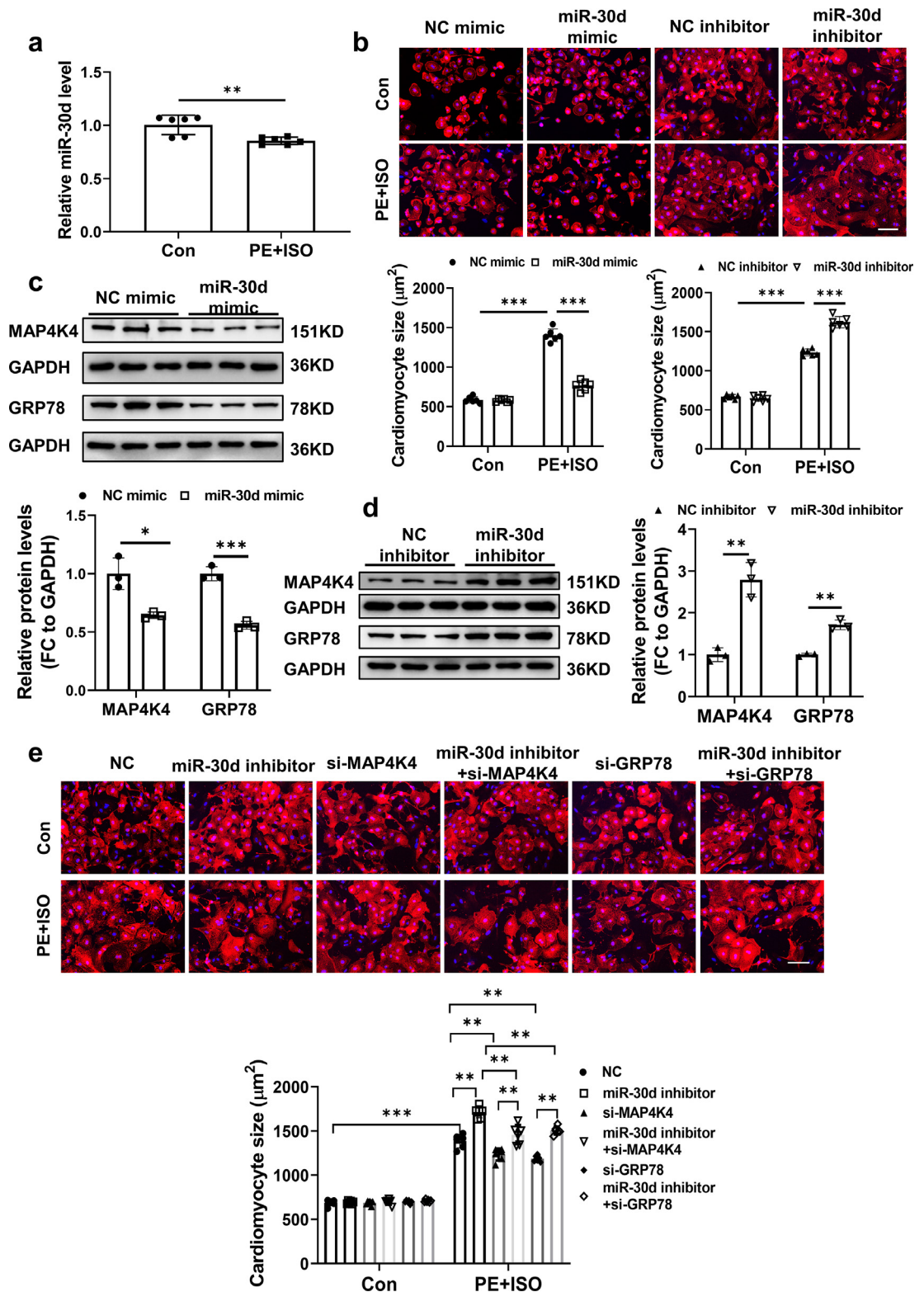


Figure 9. miR-30d protects against cardiomyocyte hypertrophy in human embryonic stem cells-derived cardiomyocytes. (a) qRT-PCR analysis of the expression of miR-30d level in human embryonic stem cells - derived cardiomyocytes hypertrophic model treated with phenylephrine (PE) and isoproterenol (ISO) ($n = 6$ per group). (b) **Upper**, Representative immunofluorescence image of

diabetic cardiomyopathy. The response of miR-30d is also different. The expression of miR-30d has been shown to be increased in diabetes. miR-30d was found to be increased in endothelial cells of the left ventricle of db/db mice, but not other organs;³⁶ increased in lactating mothers with type 1 diabetes;³⁷ increased in the serum of patients with type 2 diabetes.³⁸ Second, miR-30d was reported to be a glucose-regulated miRNA and could induce insulin transcription in pancreatic β -cells.^{39,40} Also, miR-30d was associated with insulin resistance and glucose metabolism in muscle cell.⁴¹ Thus, the elevated miR-30d in diabetic cardiomyopathy may be caused by high glucose. Third, metabolic flexibility is impaired in diabetic cardiomyopathy. The utilization of fatty acids in failing diabetic hearts was decreased.⁴² In addition, miR-30d was reported to promote fatty acid beta-oxidation in cardiac endothelium in type 2 diabetes mice.³⁶ Thus, the excessive generation of reactive lipid intermediates in cardiomyocytes may induce lipotoxicity. Without the diabetes injury, the profatty acid beta-oxidation of miR-30d may benefit cardiomyocytes. Moreover, miR-30d also participated in exercise cardioprotection from the small extracellular vesicles (sEVs) secreted by brown adipose tissue (BAT).⁴³ In this study, by using many models that used in vivo (Ang II, TAC and ISO induced mice model; ISO induced rat model) and in vitro (Ang II and PE induced NRCM model; PE and ISO induced hES-CM model), which represent different intrinsic pathways that cause cardiac hypertrophy, we show that miR-30d is a common therapeutic target for cardiac hypertrophy and heart failure. These clinical and preclinical findings highlight the potential translational of miR-30d in human pathological cardiac hypertrophy and heart failure.

Histone lysine methylation has emerged as a critical player in the regulation of gene expression. Enhancer of zeste homologue 2 (EZH2) is a crucial epigenetic regulator of gene expression. Working as methyltransferase, EZH2 adds methyl groups to histone H3 at lysine 27 and promotes the formation of heterochromatin,

resulting in repression of gene expression. In the current study, we found that EZH2 was upregulated in pathological cardiac hypertrophy models and served as an epigenetic inhibitor of miR-30d. It should be noted that EZH2 has been found to be up-regulated in multiple types of cardiovascular diseases, such as dilated cardiomyopathy, pathological cardiac hypertrophy, myocardial ischemia-reperfusion, coronary heart disease, atrial fibrosis, ischemic heart disease.⁴⁴⁻⁴⁹ H3K27me3 enrichment within the miR-30d promoter region has been reported in breast cancer cell, malignant peripheral nerve sheath tumors and brain tissues.⁵⁰⁻⁵² In our work, miR-30d was identified as a downstream target involved in the cardiac protective effect of EZH2. Here, we further demonstrated that EZH2 directly inhibits miR-30d in hypertrophic cardiomyocytes.

MAP4K4 has been identified as a target gene of miR-30d in cardiomyocyte apoptosis.^{8,53-55} However, the potential role of MAP4K4 in pathological cardiac hypertrophy is still unknown. Here, we found MAP4K4 plays a regulatory role in cardiac hypertrophy, which suggested that MAP4K4 is a tractable therapeutic target in cardiac muscle cell injury. In addition, we also identified another target gene of miR-30d in the regulation of cardiac hypertrophy. GRP78 is a target gene of miR-30d in cancer.¹⁷ Interestingly, GRP78 has been reported to enhance cardiomyocyte growth.¹⁸ Collectively, MAP4K4 and GRP78 were two target genes of miR-30d in the protection of cardiac hypertrophy. However, how MAP4K4 and GRP78 regulate cardiac hypertrophy still needs further exploration. In our study, we found MAP4K4 and GRP78 regulated cardiac hypertrophy independently rather than through interaction with each other. In addition, calcineurin-NFAT signaling plays a regulatory role in maladaptive hypertrophy and heart failure.¹⁹⁻²¹ Meanwhile, MAP4K4 and GRP78 could positively regulate the expression of NFATc3. Thus, the EZH2-miR-30d-MAP4K4/GRP78-NFAT signaling pathway appears to be involved in cardiac hypertrophy.

a-actinin (red)- and DAPI (blue)-stained human embryonic stem cells – derived cardiomyocytes transfected with miR-30d mimic, negative control (NC) mimic, miR-30d inhibitor and NC inhibitor before treated with or without PE+ISO for 48 h. Scale bar, 200 μ m; **Below**, Quantification of the average cell surface areas of PE+ISO-treated human embryonic stem cells – derived cardiomyocytes transfected with miR-30d mimic, NC mimic miR-30d inhibitor and NC inhibitor. ($n = 6$ per group, number of CM ≥ 50 cells per sample). (c) Western blot analysis and quantification of the expression of MAP4K4 and GRP78 protein level in human embryonic stem cells – derived cardiomyocytes treated with miR-30d mimic or NC mimic for 48 h ($n = 3$ per group). (d) Western blot analysis and quantification of the expression of MAP4K4 and GRP78 protein level in human embryonic stem cells – derived cardiomyocytes treated with miR-30d inhibitor or NC inhibitor for 48 h ($n = 3$ per group). (e) **Upper**, Representative immunofluorescence image of a-actinin (red)- and DAPI (blue)-stained human embryonic stem cells – derived cardiomyocytes transfected with miR-30d inhibitor and MAP4K4 siRNA or GRP78 siRNA before treated with or without PE+ISO for 48 h. Scale bar, 200 μ m. **Below**, Quantification of the average cell surface areas of embryonic stem cells – derived cardiomyocytes transfected with miR-30d inhibitor and MAP4K4 siRNA or GRP78 siRNA before treated with or without PE+ISO. ($n = 6$ per group, number of CM ≥ 50 cells per sample). Data are presented as mean \pm SD. Statistical significance was determined by Student *t* test (a, c, d) and two-way ANOVA with post hoc tukey (b, e). *, $P < 0.05$; **, $P < 0.01$ and ***, $P < 0.001$.

In conclusion, our data demonstrate that miR-30d can protect against pathological cardiac hypertrophy. Our study here provides a new therapeutic target to combat pathological cardiac hypertrophy.

Contributors

J.X. and L.Y. designed the study, instructed all experiments, and drafted the manuscript. J.L., Z.S., X.Z., W.X., W.Y., T.Y., B.J., Y.Y., R.C., S.W., and Z.W. performed the experiments and analyzed the data. J.Y., J.X., G.L. and S.D. provided technical assistance and revised the manuscript. All authors read, verified the underlying data and approved the manuscript. All authors have accessed and verified the data. J.X. and L.Y. was responsible for the decision to submit the manuscript.

Data sharing statement

The data for this study are available by contacting the corresponding author upon reasonable request.

Declaration of interests

Dr. Das is a founder of Switch Therapeutics, which did not play any role in this study and has consulted for Amgen. The other authors have declared that no conflict of interest exists.

Acknowledgements

This work was supported by the grants from National Key Research and Development Project (2018YFE0113500 to J Xiao), National Natural Science Foundation of China (82020108002 to J Xiao, 81900359 to J Li), the grant from Science and Technology Commission of Shanghai Municipality (20DZ2255400 and 21XD1421300 to J Xiao, 22010500200 to J Li), Shanghai Sailing Program (19YF1416400 to J Li), the “Dawn” Program of Shanghai Education Commission (19SG34 to J Xiao), the “Chen Guang” project supported by the Shanghai Municipal Education Commission and Shanghai Education Development Foundation (19CG45 to J Li).

Supplementary materials

Supplementary material associated with this article can be found in the online version at doi:10.1016/j.ebiom.2022.104108.

References

- Nakamura M, Sadoshima J. Mechanisms of physiological and pathological cardiac hypertrophy. *Nat Rev Cardiol.* 2018;15(7):387–407.

- Wehbe N, Nasser SA, Pintus G, Badran A, Eid AH, Baydoun E. MicroRNAs in cardiac hypertrophy. *Int J Mol Sci.* 2019;20(19):4714.
- Bei Y, Lu D, Bar C, et al. miR-486 attenuates cardiac ischemia/reperfusion injury and mediates the beneficial effect of exercise for myocardial protection. *Mol Ther.* 2022;30(4):1675–1691.
- Zeng N, Wen YH, Pan R, et al. Dickkopf 3: a novel target gene of miR-25-3p in promoting fibrosis-related gene expression in myocardial fibrosis. *J Cardiovasc Transl Res.* 2021;14(6):1051–1062.
- Abplanalp WT, Fischer A, John D, et al. Efficiency and target derepression of anti-miR-92a: results of a first in human study. *Nucleic Acid Ther.* 2020;30(6):335–345.
- Taubel J, Hauke W, Rump S, et al. Novel antisense therapy targeting microRNA-132 in patients with heart failure: results of a first-in-human Phase 1b randomized, double-blind, placebo-controlled study. *Eur Heart J.* 2021;42(2):178–188.
- Melman YF, Shah R, Danielson K, et al. Circulating MicroRNA-30d is associated with response to cardiac resynchronization therapy in heart failure and regulates cardiomyocyte apoptosis: a translational pilot study. *Circulation.* 2015;131(25):2202–2216.
- Li J, Salvador AM, Li G, et al. Mir-30d regulates cardiac remodeling by intracellular and paracrine signaling. *Circ Res.* 2021;128(1):e1–e23.
- Zhou Q, Pan LL, Xue R, et al. The anti-microbial peptide LL-37/CRAMP levels are associated with acute heart failure and can attenuate cardiac dysfunction in multiple preclinical models of heart failure. *Theranostics.* 2020;10(14):6167–6181.
- Liu X, Xiao J, Zhu H, et al. miR-222 is necessary for exercise-induced cardiac growth and protects against pathological cardiac remodeling. *Cell Metab.* 2015;21(4):584–595.
- Li J, Yang T, Tang H, et al. Inhibition of lncRNA MAAT controls multiple types of muscle atrophy by cis- and trans-regulatory actions. *Mol Ther.* 2021;29(3):1102–1119.
- Li J, Yang T, Sha Z, et al. Angiotensin II-induced muscle atrophy via PPARgamma suppression is mediated by miR-29b. *Mol Ther Nucleic Acids.* 2021;23:743–756.
- Xiao J, Gao R, Bei Y, et al. Circulating miR-30d predicts survival in patients with acute heart failure. *Cell Physiol Biochem.* 2017;41(3):865–874.
- Wang H, Maimaitiaili R, Yao J, et al. Percutaneous intracoronary delivery of plasma extracellular vesicles protects the myocardium against ischemia-reperfusion injury in canis. *Hypertension.* 2021;78(5):1541–1554.
- Tohyama S, Hattori F, Sano M, et al. Distinct metabolic flow enables large-scale purification of mouse and human pluripotent stem cell-derived cardiomyocytes. *Cell Stem Cell.* 2013;12(1):127–137.
- Bei Y, Lu D, Bar C, et al. miR-486 attenuates cardiac ischemia/reperfusion injury and mediates the beneficial effect of exercise for myocardial protection. *Mol Ther.* 2022;30(4):1675–1691.
- Su SF, Chang YW, Andreu-Vieyra C, et al. miR-30d, miR-181a and miR-199a-5p cooperatively suppress the endoplasmic reticulum chaperone and signaling regulator GRP78 in cancer. *Oncogene.* 2013;32(39):4694–4701.
- Zhang G, Wang X, Bi X, et al. GRP78 (glucose-regulated protein of 78 kDa) promotes cardiomyocyte growth through activation of GATA4 (GATA-binding protein 4). *Hypertension.* 2019;73(2):390–398.
- Molkentin JD. Calcineurin and beyond: cardiac hypertrophic signaling. *Circ Res.* 2000;87(9):731–738.
- Wilkins BJ, Dai YS, Bueno OF, et al. Calcineurin/NFAT coupling participates in pathological, but not physiological, cardiac hypertrophy. *Circ Res.* 2004;94(1):110–118.
- MacDonnell SM, Weisser-Thomas J, Kubo H, et al. CaMKII negatively regulates calcineurin-NFAT signaling in cardiac myocytes. *Circ Res.* 2009;105(4):316–325.
- Lu D, Thum T. RNA-based diagnostic and therapeutic strategies for cardiovascular disease. *Nat Rev Cardiol.* 2019;16(11):661–674.
- Ling H, Fabbri M, Calin GA. MicroRNAs and other non-coding RNAs as targets for anticancer drug development. *Nat Rev Drug Discov.* 2013;12(11):847–865.
- Bernardo BC, Ooi JY, Lin RC, McMullen JR. miRNA therapeutics: a new class of drugs with potential therapeutic applications in the heart. *Future Med Chem.* 2015;7(13):1771–1792.
- Wu M, Wang G, Tian W, Deng Y, Xu Y. MiRNA-based therapeutics for lung cancer. *Curr Pharm Des.* 2018;23(39):5989–5996.
- Chen F, Ye X, Jiang H, Zhu G, Miao S. MicroRNA-151 attenuates apoptosis of endothelial cells induced by oxidized low-density

- lipoprotein by targeting interleukin-17A (IL-17A). *J Cardiovasc Transl Res*. 2021;14(3):400–408.
- 27 Liu Q, Chen L, Liang X, et al. Exercise attenuates angiotensin-induced muscle atrophy by targeting PPARgamma/miR-29b. *J Sport Health Sci*. 2021. <https://doi.org/10.1016/j.jshs.2021.06.002>.
 - 28 Torma F, Gombos Z, Jokai M, et al. The roles of microRNA in redox metabolism and exercise-mediated adaptation. *J Sport Health Sci*. 2020;9(5):405–414.
 - 29 Chen D, Guo W, Qiu Z, et al. MicroRNA-30d-5p inhibits tumour cell proliferation and motility by directly targeting CCNE2 in non-small cell lung cancer. *Cancer Lett*. 2015;362(2):208–217.
 - 30 Croset M, Pantano F, Kan CWS, et al. miRNA-30 family members inhibit breast cancer invasion, osteomimicry, and bone destruction by directly targeting multiple bone metastasis-associated genes. *Cancer Res*. 2018;78(18):5259–5273.
 - 31 Liang L, Yang Z, Deng Q, et al. miR-30d-5p suppresses proliferation and autophagy by targeting ATG5 in renal cell carcinoma. *FEBS Open Bio*. 2021;11(2):529–540.
 - 32 Morishima M, Ono K. Serum microRNA-30d is a sensitive biomarker for angiotensin II-induced cardiovascular complications in rats. *Heart Vessels*. 2021;36(10):1597–1606.
 - 33 Bao J, Lu Y, She Q, et al. MicroRNA-30 regulates left ventricular hypertrophy in chronic kidney disease. *JCI Insight*. 2021;6(10):e138027.
 - 34 Ro WB, Kang MH, Song DW, Lee SH, Park HM. Expression profile of circulating MicroRNAs in dogs with cardiac hypertrophy: a pilot study. *Front Vet Sci*. 2021;8: 652224.
 - 35 Li X, Du N, Zhang Q, et al. MicroRNA-30d regulates cardiomyocyte pyroptosis by directly targeting foxo3a in diabetic cardiomyopathy. *Cell Death Dis*. 2014;5:e1479.
 - 36 Veitch S, Njock MS, Chandy M, et al. MiR-30 promotes fatty acid beta-oxidation and endothelial cell dysfunction and is a circulating biomarker of coronary microvascular dysfunction in pre-clinical models of diabetes. *Cardiovasc Diabetol*. 2022;21(1):31.
 - 37 Frorup C, Mirza AH, Yarani R, et al. Plasma exosome-enriched extracellular vesicles from lactating mothers with type 1 diabetes contain aberrant levels of miRNAs during the postpartum period. *Front Immunol*. 2021;12:744509.
 - 38 Kong L, Zhu J, Han W, et al. Significance of serum microRNAs in pre-diabetes and newly diagnosed type 2 diabetes: a clinical study. *Acta Diabetol*. 2011;48(1):61–69.
 - 39 Zhao X, Mohan R, Ozcan S, Tang X. MicroRNA-30d induces insulin transcription factor MafA and insulin production by targeting mitogen-activated protein kinase 4 (MAP4K4) in pancreatic beta-cells. *J Biol Chem*. 2012;287(37):31155–31164.
 - 40 Tang X, Muniappan L, Tang G, Ozcan S. Identification of glucose-regulated miRNAs from pancreatic {beta} cells reveals a role for miR-30d in insulin transcription. *RNA*. 2009;15(2):287–293.
 - 41 Zhou T, Meng X, Che H, et al. Regulation of insulin resistance by multiple MiRNAs via targeting the GLUT4 signalling pathway. *Cell Physiol Biochem*. 2016;38(5):2063–2078.
 - 42 Phang RJ, Ritchie RH, Hausenloy DJ, Lees JG, Lim SY. Cellular interplay between cardiomyocytes and non-myocytes in diabetic cardiomyopathy. *Cardiovasc Res*. 2022. <https://doi.org/10.1093/cvr/cvaco49>.
 - 43 Zhao H, Chen X, Hu G, et al. Small extracellular vesicles from brown adipose tissue mediate exercise cardioprotection. *Circ Res*. 2022;130(10):1490–1560.
 - 44 Tschirner A, Palus S, Hetzer R, Meyer R, Anker SD, Springer J. Sixi is down-regulated in end-stage human dilated cardiomyopathy independently of Ezh2. *ESC Heart Fail*. 2014;1(2):154–159.
 - 45 Dong W, Xie F, Chen XY, et al. Inhibition of Smurf2 translation by miR-322/503 protects from ischemia-reperfusion injury by modulating EZH2/Akt/GSK3beta signaling. *Am J Physiol Cell Physiol*. 2019;317(2):C253–C261.
 - 46 Gao W, Guo N, Zhao S, et al. FBXW7 promotes pathological cardiac hypertrophy by targeting EZH2-SIX1 signaling. *Exp Cell Res*. 2020;393(1):112059.
 - 47 Liu Y, Dai C, Lei Y, Wu W, Liu W. Inhibition of EZH2 attenuates coronary heart disease by interacting with microRNA-22 to regulate the TXNIP/nuclear factor-kappaB pathway. *Exp Physiol*. 2020;105(12):2038–2050.
 - 48 Song S, Zhang R, Mo B, et al. EZH2 as a novel therapeutic target for atrial fibrosis and atrial fibrillation. *J Mol Cell Cardiol*. 2019;135:119–133.
 - 49 Zhao L, You T, Lu Y, Lin S, Li F, Xu H. Elevated EZH2 in ischemic heart disease epigenetically mediates suppression of Nav1.5 expression. *J Mol Cell Cardiol*. 2021;153:95–103.
 - 50 Yin H, Wang Y, Wu Y, et al. EZH2-mediated epigenetic silencing of miR-29/miR-30 targets LOXL4 and contributes to tumorigenesis, metastasis, and immune microenvironment remodeling in breast cancer. *Theranostics*. 2020;10(19):8494–8512.
 - 51 Zhang P, Garnett J, Creighton CJ, et al. EZH2-miR-30d-KPNB1 pathway regulates malignant peripheral nerve sheath tumour cell survival and tumourigenesis. *J Pathol*. 2014;232(3):308–318.
 - 52 Jin D, Wei W, Song C, Han P, Leng X. Knockdown EZH2 attenuates cerebral ischemia-reperfusion injury via regulating microRNA-30d-3p methylation and USP22. *Brain Res Bull*. 2021;169:25–34.
 - 53 Fiedler LR, Chapman K, Xie M, et al. MAP4K4 inhibition promotes survival of human stem cell-derived cardiomyocytes and reduces infarct size in vivo. *Cell Stem Cell*. 2019;24(4):579–591.e12.
 - 54 Golorfoush PA, Narasimhan P, Chaves-Guerrero PP, et al. Selective protection of human cardiomyocytes from anthracycline cardiotoxicity by small molecule inhibitors of MAP4K4. *Sci Rep*. 2020;10(1):12060.
 - 55 Te Lintel Hekkert M, Newton G, Chapman K, et al. Preclinical trial of a MAP4K4 inhibitor to reduce infarct size in the pig: does cardioprotection in human stem cell-derived myocytes predict success in large mammals? *Basic Res Cardiol*. 2021;116(1):34.